HAWAII GEOTHERMAL PROJECT

ENGINEERING PROGRAM

QUARTERLY REPORT No. 4

SEPTEMBER 16, 1974

Prepared Under

NATIONAL SCIENCE FOUNDATION

RESEARCH GRANT NO. GI-38319

By

Hi Chang Chai
Bill Chen
Ping Cheng
James Chou
Deane Kihara
Kah Hie Lau
L. Stephen Lau
Patrick Takahashi
Paul Yuen

Hilo College
University of Hawaii
Hilo, Hawaii 96720

College of Engineering
University of Hawaii
Honolulu, Hawaii 96822

Table of Contents

Page

INTRODUCTION 1

TASK 3.1 GEOTHERMAL RESERVOIR ENGINEERING

A. Timetable 2

B. Progress to Date 5

C. Future Work 20

D. References 21

TASK 3.6 OPTIMAL GEOTHERMAL PLANT DESIGN

A. Timetable 22

B. Progress to Date 23

C. Future Work 57

D. References 58

HAWAII GEOTHERMAL PROJECT

ENGINEERING PROGRAM

QUARTERLY REPORT NO. 4

September 16, 1974

INTRODUCTION

The objectives of the Engineering Program are (1) applied research in problem areas related to the extraction of energy from geothermal resources, and (2) planning, design, and specification of a research-oriented, environmentally-acceptable geothermal power plant. Work is progressing on two tasks:

Task 3.1 Geothermal Reservoir Engineering
Task 3.6 Optimal Geothermal Plant Design

This report summarizes the timetable (A) for each task, the progress made to date (B), and the future work planned (C).

TASK 3.1 GEOTHERMAL RESERVOIR ENGINEERING

A. Timetable

1. Numerical Modelling of Geothermal Reservoirs

Investigators: P. Cheng, K. H. Lau, and L. S. Lau

August 15, 1973	1. Survey literature on the Ghyben-Herzberg lens dynamics with emphasis on coning and steady flow with heat source below 2. Survey literature on building a physical model to simulate the Ghyben-Herzberg lens system
December 31, 1973	1. Formulate convection problem for a rectangular porous region 2. Solve convection problem for a rectangular region using finite difference method 3. Formulate coning problem
May 31, 1974	1. Complete problem of free convection in an unconfined geothermal reservoir 2. Complete survey of literature on the numerical solution of pumping and reinjection in an aquifer under isothermal conditions
December 31, 1974	1. Complete investigation of the effect of vertical heat source on the upwelling of the water table 2. Formulate finite element solution of free convection in a geothermal reservoir with irregular geometry
May 31, 1975	1. Complete investigation of the effects of geothermal heating on Ghyben-Herzberg lens 2. Complete numerical solutions for heat transfer and fluid flow characteristics in an axisymmetric geothermal reservoir 3. Complete numerical solution of steady state pumping and reinjection in a confined geothermal reservoir
December 31, 1975	1. Complete finite element solution of free convection in a two-dimensional geothermal reservoir with irregular geometry 2. Formulate problem of transient responses in geothermal reservoirs with pumping and reinjection

2. Well Test Analysis and Physical Modelling

Investigators: P. Takahashi, B. Chen, and L. S. Lau

May 19, 1973	1. Study gas and petroleum well test analysis
June-July-August, 1973	1. Study nature of a geothermal reservoir and geothermal well testing
July-August, 1973	1. Initiate international survey on the state of Geothermal Reservoir Engineering
August 31, 1973	1. Continue study on reservoir and well test analysis 2. Analyze international survey results
December 31, 1973	1. Perform research on the construction of a geothermal reservoir model 2. Design preliminary model 3. Continue research on geothermal reservoirs and well testing (with Geophysics Program) 4. Investigate whether a typical Hawaii geothermal reservoir is an open or a closed system
May, 1974	1. Assess well test hardware 2. Complete analysis of international survey results 3. Design physical geothermal reservoir model 4. Continue research on geothermal reservoirs and well testing (with Geophysics Program)
December, 1974	1. Select hardware for well testing 2. Assess software for well testing 3. Complete initial phase of the fabrication of the physical model 4. Develop well test analysis methodology in conjunction with Geophysics Drilling Program 5. Initiate computer program on well test analysis
May, 1975	1. Purchase hardware and select software for well testing (with Geophysics Program) 2. Initiate laboratory parametric checks 3. Assess methods for measurement and analysis of two-phase flow 4. Design Ghyben-Herzberg lens physical model 5. Develop computer program to combine type curve matching and mass/energy balance into a single predictive tool
September, 1975	1. Initiate laboratory simulation studies 2. Fabricate Ghyben-Herzberg lens physical model 3. Purchase equipment to interface the different physical models

December, 1975	1. Analyze laboratory simulation runs and correlate with computer model 2. Interface physical models into a general model of a geothermal field 3. Develop methods for two-phase flow measurement and analysis 4. Measure temperature, pressure and flow rate--both donwhole and at wellhead 5. Analyze data
December, 1976	1. Complete analysis of geothermal well data 2. Predict geothermal field performance

B. Progress to Date

Research in geothermal reservoir engineering, Task 3.1, has continued in the areas of numerical modelling, geothermal fluid flow characterization, well test analysis, and physical modelling. The emphases during this quarter were in the first three areas.

1. Numerical Modelling of Geothermal Reservoirs

During the past three months, work has been performed on the following four problems.

a. The Effects of Dike Intrusion on the Upwelling of Water Table

The purpose of the analysis is to assess in a qualitative manner whether the upwelling of water table of 2000 feet above sea level reported by Keller [private communication] is due to vertical heat sources.

Suppose a dike exists in the reservoir as shown in Fig. 3.1-1A with the idealized situation shown in Fig. 3.1-1B. The governing equations are given in Ref. [1]. In addition to boundary conditions given in Ref. [1], the boundary conditions on the dike are

$$\theta(X_{S_1},Y) = \theta_S \ , \qquad Y \leq Y_S \qquad (1a)$$

$$\theta(X_{S_2},Y) = \theta_S \ , \qquad Y \leq Y_S \qquad (1b)$$

$$\frac{\partial P}{\partial X}(X_{S_1},Y) = 0 \ , \qquad Y \leq Y_S \qquad (1c)$$

$$\frac{\partial P}{\partial X}(X_{S_2},Y) = 0 \ , \qquad Y \leq Y_S \qquad (1d)$$

$$\frac{\partial P}{\partial X}(X,Y_S) = -1 + \varepsilon\theta_S \ , \qquad X_{S_1} \leq X \leq X_{S_2} \qquad (1e)$$

$$\theta(X,Y_S) = \theta_S \ , \qquad X_{S_1} \leq X \leq X_{S_2} \qquad (1f)$$

where θ_S is the prescribed dimensionless temperature of the dike. As a result of the perturbation technique described earlier, a set of linear equations is obtained. The resultant equations can then be solved numerically based on the finite difference method. Computations were carried out for the following two cases:

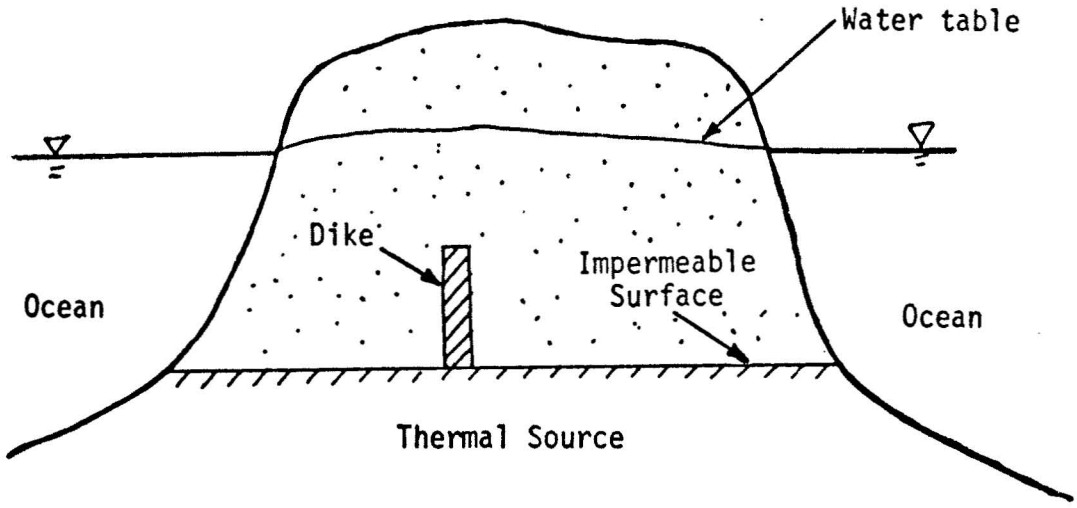

FIG. 3.1-1A UNCONFINED AQUIFER WITH A VERTICAL DIKE

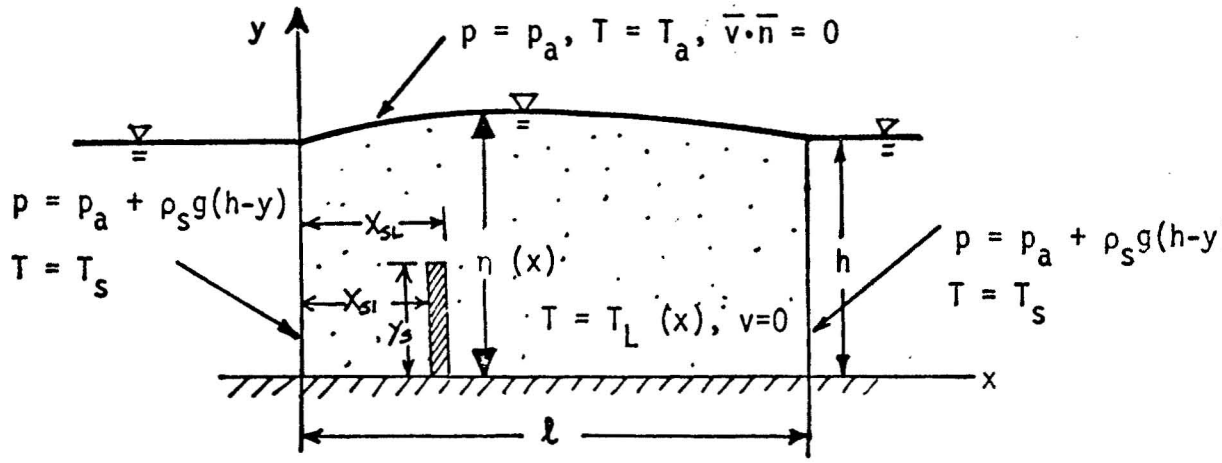

FIG. 3.1-1B IDEALIZED RECTANGULAR MODEL OF AQUIFER WITH A VERTICAL DIKE

A. Vertical heating only

$$\theta_S = 1 , \qquad 0 \leq Y \leq 0.5 ,$$

B. Horizontal and vertical heating

$$\theta_L(X) = \exp[-(\frac{X-2}{0.5})^2] , \qquad 0 < X < 1.9, \quad 2.2 < X < 4$$

$$\theta_S = 1 , \qquad 0 \leq Y \leq 0.5, \quad 1.9 \leq X \leq 2.1$$

Results of these computations along with previous results for horizontal heating are compared in Figs. 3.1-2, 3.1-3, and 3.1-4. Fig. 3.1-2 shows the contours of stream functions for Cases A, B, and C where C referred to the previous results obtained in Ref. [1]. It is shown that the stream functions of the three cases exhibit similar behavior. The comparison of temperature contours for the three cases with D = 500 and ε = 0.1 are plotted in Fig. 3.1-3 where it is shown that hot water at shallow depth is possible whenever there is a hot vertical heat source. The effects of vertical and horizontal heating on the upwelling of water table are shown in Fig. 3.1-4 where it is shown that the amount of upwelling increases for a vertical heat source. However, the upwelling of 2000 feet seems to be unlikely. A manuscript covering this work is now under preparation, and will be submitted for publication in a journal.

b. Heat Transfer and Fluid Flow Characteristics in an Axisymmetric Geothermal Reservoir

To have a qualitative understanding of the three-dimensional effects of seepage from the ocean on the temperature distribution in geothermal reservoirs, a study has been undertaken for the idealized case of an axisymmetric cylindrical configuration. The formulation of the problem is similar to that given in Ref. [1] except that governing equations and boundary conditions are written in cylindrical coordinates. Numerical computations for L = 4, D = 500, and ε = 0.1 were carried out. The comparison of temperature contours and vertical temperature profiles between an axisymmetric cylindrical reservoir and a rectangular one is shown in Fig. 3.1-5 and 3.1-6 where solid lines are for axisymmetric reservoirs and dotted lines are for rectangular ones. It is shown in these figures that temperature in a rectangular reservoir is considerably higher than that in an axisymmetric

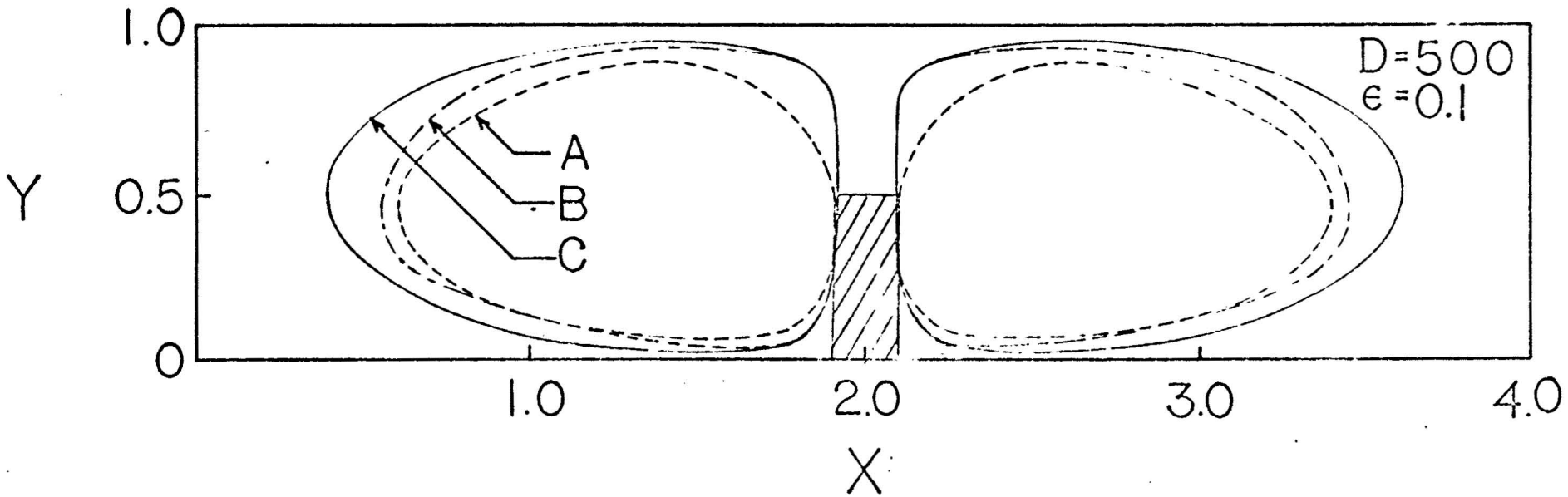

FIG. 3.1-2 EFFECTS OF VERTICAL AND HORIZONTAL HEATING ON STREAM LINES

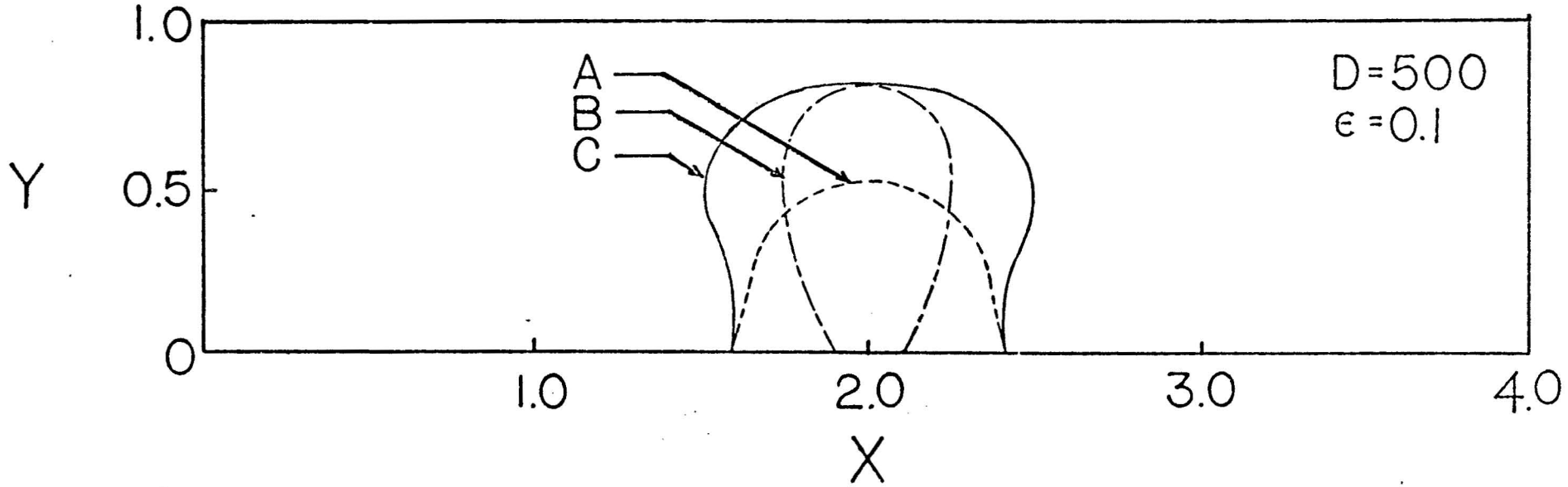

FIG. 3.1-3 EFFECTS OF VERTICAL AND HORIZONTAL HEATING ON TEMPERATURE CONTOURS

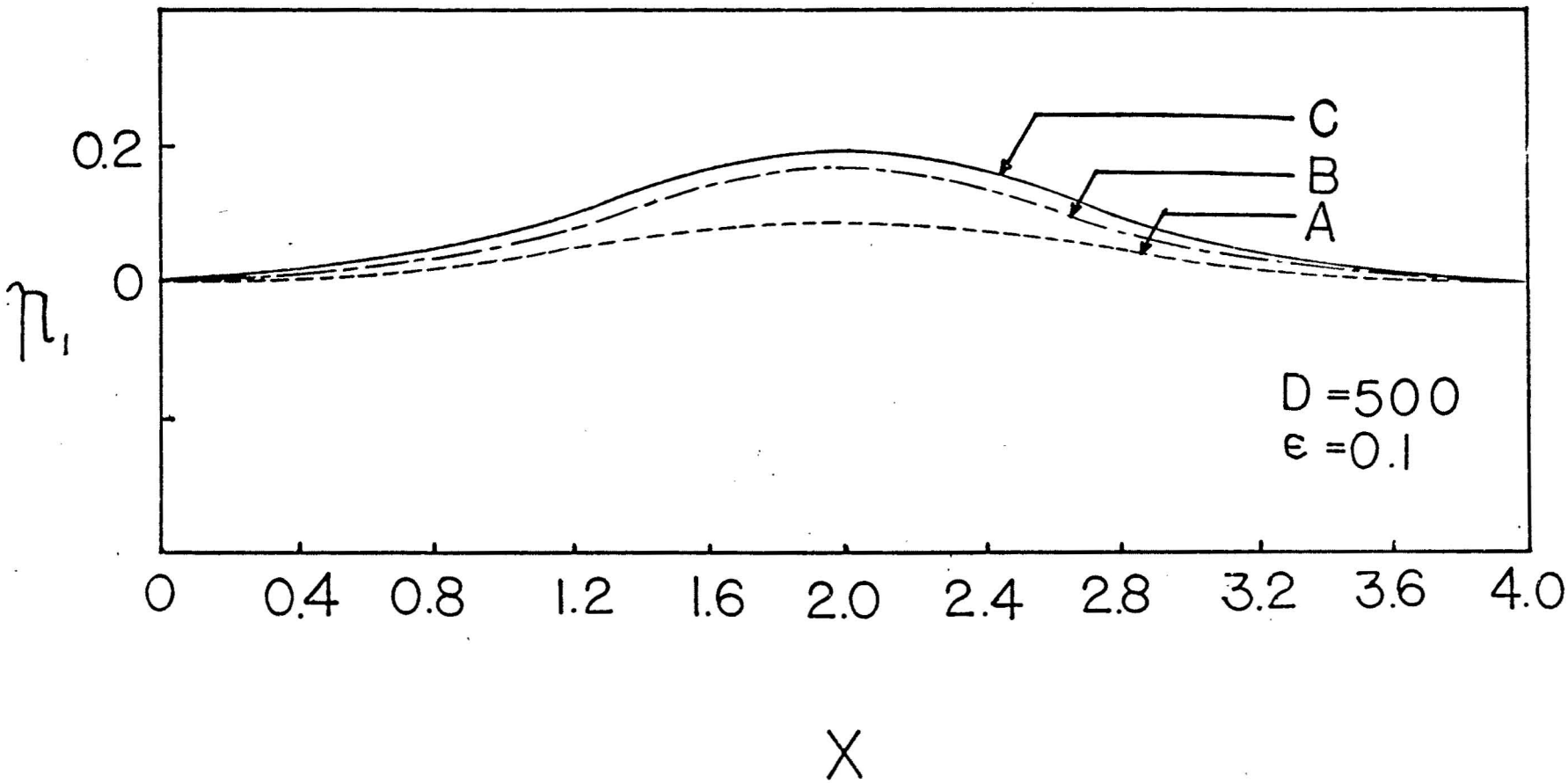

FIG. 3.1-4 EFFECTS OF VERTICAL AND HORIZONTAL HEATING ON THE FIRST-ORDER PERTURBATION FUNCTION FOR THE UPWELLING OF WATER TABLE

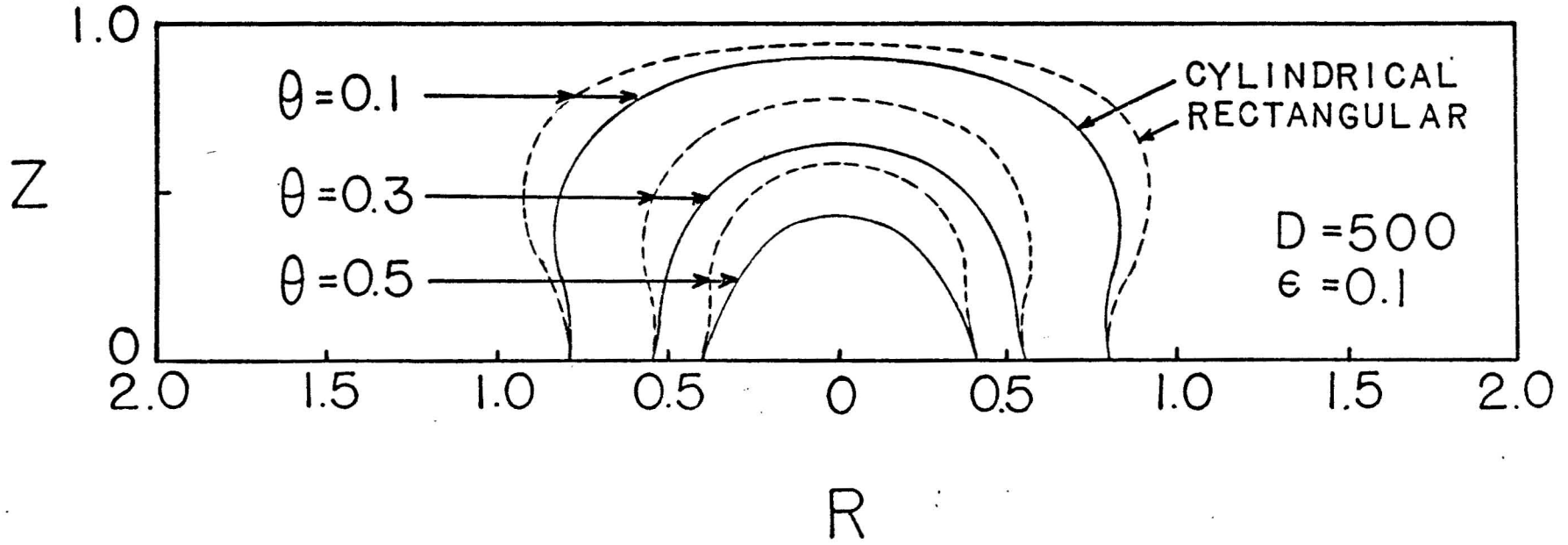

FIG. 3.1-5 EFFECT OF CONFIGURATION OF RESERVOIR ON TEMPERATURE CONTOURS

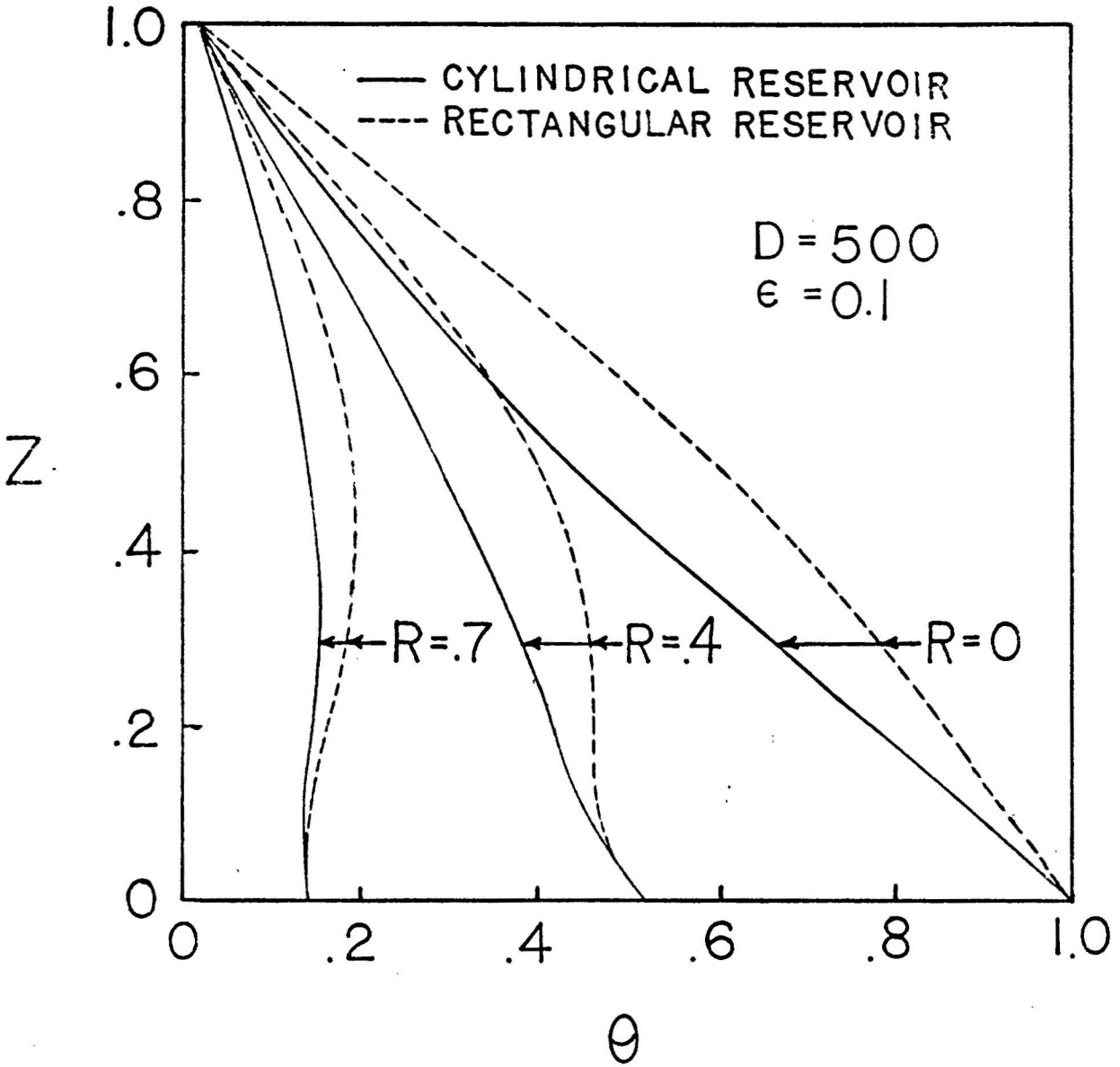

FIG. 3.1-6 EFFECT OF CONFIGURATION OF RESERVOIR ON VERTICAL TEMPERATURE PROFILES

reservoir due to the three-dimensional seepage effect. Consequently, the upwelling of water table due to geothermal heating is smaller for axisymmetric reservoirs than that of rectangular reservoirs as is shown in Fig. 3.1-7.

c. Steady Pumping and Reinjection in a Hot-Brine Reservoir

Pumping and reinjection of fluids will undoubtedly influence the temperature distribution in a geothermal reservoir, especially in a region near the coast. For a rectangular confined reservoir with a pumping well located at (x_1,y_1) at a pumping rate of Q_1, and a reinjection well at (x_2, y_2) with a reinjection rate of Q_2, it can be shown that the governing dimensionless equations are

$$\frac{\partial^2 P}{\partial X^2} + \frac{\partial^2 P}{\partial Y^2} - \varepsilon \frac{\partial \theta}{\partial Y} = \bar{Q}_1 \delta(X-X_1)\delta(Y-Y_1) - \bar{Q}_2 \delta(X-X_2)\delta(Y-Y_2) \quad , \tag{2a}$$

$$\frac{\partial^2 \theta}{\partial X^2} + \frac{\partial^2 \theta}{\partial Y^2} + D\left\{\frac{\partial P}{\partial X}\frac{\partial \theta}{\partial X} + \frac{\partial P}{\partial Y}\frac{\partial \theta}{\partial Y} + [1-\varepsilon(\theta-\theta_s)]\frac{\partial \theta}{\partial Y}\right\} = 0 \quad , \tag{2b}$$

where

δ's are the delta functions, $\quad \varepsilon \equiv \beta T_c$, $\quad \theta \equiv \frac{T}{T_c}$,

$$\bar{Q}_1 \equiv \frac{Q_1}{\frac{\rho_s K g}{\mu}} , \quad \bar{Q}_2 \equiv \frac{Q_2}{\frac{\rho_s K g}{\mu}} , \quad P \equiv \frac{p-p_a}{\rho_s g h} , \quad D \equiv \frac{\rho_s K g h}{\alpha \mu} , \tag{3}$$

$$X \equiv \frac{x}{h} , \quad Y \equiv \frac{y}{h} , \quad \theta_s \equiv \frac{T_s}{T_c} ,$$

with the subscripts "s", "a", and "c" denoting the conditions in the ocean, in the atmosphere, and at the maximum temperature of the impermeable surface. The quantities ρ, μ, β in Eq. (3) are the density, viscosity, thermal expansion coefficient of the fluid whereas α and K are the thermal diffusivity and the permeability of the medium.

Boundary conditions along the ocean are

$$P(0,Y) = P(L,Y) = 1 - Y \quad , \tag{4a}$$

$$\theta(0,Y) = \theta(L,Y) = \theta_s \quad . \tag{4b}$$

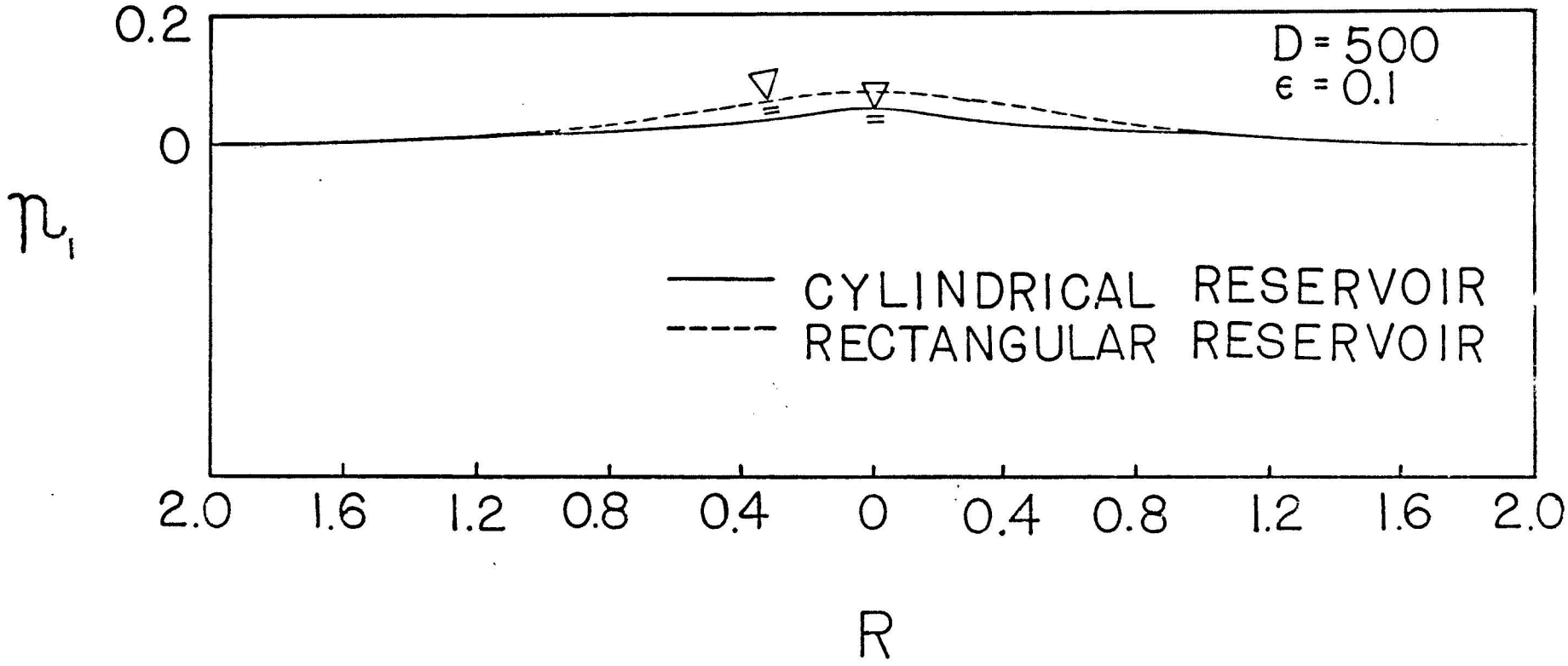

FIG. 3.1-7 EFFECT OF CONFIGURATION OF RESERVOIR ON THE FIRST-ORDER PERTURBATION FUNCTION FOR THE UPWELLING OF WATER TABLE

Along the impermeable surfaces at Y = 0, & Y = 1, the boundary conditions are

$$\frac{\partial P}{\partial Y}(X,0) = \frac{\partial P}{\partial Y}(X,1) = -1+\varepsilon(\theta_L-\theta_S) , \tag{5a}$$

$$\theta(X,0) = \theta_L(X) , \tag{5b}$$

$$\theta(X,1) = \theta_a \quad . \tag{5c}$$

If a power series in terms of ε for P & θ are substituted into Eqs. (1-5) and terms of like power in ε are collected, we have a set of linear sub-problems that can be solved numerically based on the finite difference method. The numerical solution of the problem is now in progress.

d. The Dynamics of Ghyben-Herzberg Lens

In the Hawaiian Islands, the rain percolating through the ground will form a Ghyben-Herzberg lens of fresh water which rests on top of a sea water zone. The analysis of the dynamics of the Ghyben-Herzberg lens as a result of geothermal heating will be of fundamental interest. If the fresh water and sea water are assumed to be miscible, it can be shown that the governing equations in terms of dimensionless pressure, temperature, and concentration are given by

$$\frac{\partial^2 P}{\partial X^2} + \frac{\partial^2 P}{\partial Y^2} = \varepsilon_T \frac{\partial \theta}{\partial Y} - \varepsilon_c \frac{\partial C}{\partial Y} \quad , \tag{6}$$

$$\frac{\partial^2 \theta}{\partial X^2} + \frac{\partial^2 \theta}{\partial Y^2} + D_T \left[\frac{\partial P}{\partial X}\frac{\partial \theta}{\partial X} + \frac{\partial P}{\partial Y}\frac{\partial \theta}{\partial Y}\right] + D_T \left[1-\varepsilon_T(\theta-\theta_S)+\varepsilon_c(C-1)\right] \frac{\partial \theta}{\partial Y} = 0 \quad , \tag{7}$$

$$\frac{\partial^2 C}{\partial X^2} + \frac{\partial^2 C}{\partial Y^2} + D_c \left[\frac{\partial P}{\partial X}\frac{\partial C}{\partial X} + \frac{\partial P}{\partial Y}\frac{\partial C}{\partial Y}\right] + D_c \left[1-\varepsilon_T(\theta-\theta_S)+\varepsilon_c(C-1)\right] \frac{\partial C}{\partial Y} = 0 \quad , \tag{8}$$

where P, X, and Y are defined in Eq. (3) and

$$C \equiv \frac{c}{C_s} , \quad \varepsilon_T \equiv \beta_T T_c , \quad \varepsilon_c \equiv \beta_c C_s , \quad D_T \equiv \frac{\rho_s K g h}{\alpha \mu} , \tag{9}$$

$$D_c \equiv \frac{\rho_s K g h}{\alpha_c \mu} \quad .$$

Boundary conditions along the ocean are given by

$$P(0,Y) = P(L,Y) = 1-Y \ , \tag{10a}$$

$$\theta(0,Y) = \theta(L,Y) = \theta_s \ , \tag{10b}$$

$$C(0,Y) = C(L,Y) = 1 \ . \tag{10c}$$

Along the impermeable surface, the boundary conditions are

$$\frac{\partial P}{\partial Y}(X,0) = -1+\varepsilon_T(\theta_L-\theta_s)-\varepsilon_c(C-1) \ , \tag{11a}$$

$$\theta(X,0) = \theta_L(X) \ , \tag{11b}$$

$$\frac{\partial C}{\partial Y}(X,0) = 0 \ . \tag{11c}$$

Along the free surface $Y=\bar{\eta}$, the boundary conditions are

$$\frac{\partial P}{\partial X}\frac{\partial \bar{\eta}}{\partial X} - \left[\frac{\partial P}{\partial Y} + 1 - \varepsilon_T(\theta_a-\theta_s)-\varepsilon_c\right] - \varepsilon_n = 0 \ , \tag{12a}$$

$$P(X,\bar{\eta}) = 0 \ , \tag{12b}$$

$$\theta(X,\bar{\eta}) = \theta_a \ , \tag{12c}$$

$$C(X,\bar{\eta}) = 0 \ , \tag{12d}$$

where $\varepsilon_n = \frac{\mu N}{K\rho_s g}$ with N denoting the amount of accretion at the water table. Since ε_T, ε_c, and ε_n are small, the problems can be simplified on the basis of the perturbation method with ε_T, ε_c, and ε_n as the perturbation parameters. The resultant zero-order and first-order problems are also linear and can be solved numerically using the finite difference method. The numerical solution of the problem is now in progress.

2. Well Test Analysis and Physical Modelling

a. Analysis of Well Flow Characteristics

During the past quarter a preliminary study on the effect of salinity of a two-phase flow up in a well has been completed. The essence of this study will be abstracted here; a detailed treatment will be presented in the next quarterly report.

As Hawaii geothermal reservoirs are expected to be liquid dominated and brackish (see Technical Report #3), it is essential that the basic flow characteristics of hot water wells be established. However, as geothermal

fluids vary drastically in salt content--from nearly pure water to 30% solids by weight--a generalized fluid flow analysis is not possible.

A computer program was developed to produce curves on:

1. wellhead pressure vs. flow rate,
2. vapor pressure vs. temperature,
3. Specific volume vs. temperature,
4. enthalpy vs. temperature,
5. heat of vaporization vs. temperature,
6. the effect of seawater concentration on flow rate,
7. the effect of fixed and variable friction factors on flow rate, and
8. the effect of CO_2 concentration on flow rate.

In summary: 1) flow rate decreases with increasing salinity, 2) vapor pressure, specific volume, and enthalpy increase with increasing temperature, 3) at a given temperature, vapor pressure, specific volume, and enthalpy decrease with increasing salinity, 4) heat of vaporization decreases with increasing temperature and is virtually unaffected by salinity change.

b. Well Test Analysis: A Literature Survey

A comprehensive literature survey plus the contents of two short courses on petroleum reservoir engineering and well test analysis was condensed into a resource paper on geothermal well test analysis methods. The report itself can be obtained as Hawaii Geothermal Project Technical Memorandum No. 2 [3]. A very short summary of this 40-page document will be presented here.

The report assumes that there is little or no net heat transfer across the boundaries of a geothermal reservoir. This thermodynamic system allows immediate extension of petroleum well analysis techniques into geothermal reservoir engineering. In future discussions, it should be remembered that the geothermal reservoir under consideration is thus a sealed one, and because of the relatively low thermal conductivity of rock, isothermal. Future extensions will attempt to treat non-isothermal conditions.

In order to evaluate the geothermal reservoir, be it at the drilling, development or production stage, the geothermal engineer must have data on the various parameters vital to its analysis. These data include formation thickness, permeability, porosity, viscosity, compressibility, thermal conductivity, fluid and rock density, temperature and most of all formation average pressure.

Broadly speaking, average reservoir pressures are used for characterizing a reservoir, computing its geothermal liquids in place and predicting future behavior. In characterizing a reservoir, pressures are used to relate the amount of production in a given interval of time to the pressure drop. For example, if the pressure drop is large for a given amount of production, this may indicate drainage from a small reservoir or poor permeability.

In addition to this semi-quantitative use, pressures find a quantitative use in materials-heat balance calculation of geothermal liquid in place. Thus the characteristic of the reservoir--be it compressed liquid, saturated liquid and steam or superheated steam--can be determined. Extrapolation into the future is best made by using the method which relates future production to future average pressure and materials-heat balance analysis.

From the above discussion, we see that pressure, temperature and flow measurements are vital to the evaluation and prediction of a geothermal reservoir. Therefore, every single well must have a complete and comprehensive program to secure and analyze all these measurements.

It is well known that the governing equation for pressure of a slightly compressible fluid in an isothermal one-dimensional reservoir is given by

$$\frac{1}{r}\frac{\partial}{\partial r}\left(r\frac{\partial p}{\partial r}\right) = \frac{\phi\mu c_t}{k}\frac{\partial p}{\partial t}$$

where r, p, ϕ, μ, c_t, k, and t denote distance in the radial direction, pressure, formation porosity, fluid viscosity, total system compressibility, formation permeability, and time. With the appropriate boundary conditions, solutions can be obtained. In general, curves of p_D vs. $\frac{t_D}{r_D^2}$ are obtained for varying r_D's, where

$$P_D = \frac{2\pi kh}{q\mu}\left(p_i - p_{r,t}\right)$$

$$t_D = \frac{kt}{\phi\mu c_t r_w^2}$$

$$r_D = \frac{r}{r_w}$$

with h, q, p_i, $p_{r,t}$, and r_w denoting the formation thickness, flow rate, initial formation pressure, real pressure, and radius of the producing well. These curves can be used to run interference tests, that is, how the

production of one well causes a detectable pressure drop at an adjacent well. To perform the interference test data analysis, type curve matching is utilized.

The procedure for the interference data analysis is as follows:

1. Graph the pressure drop at the observation well vs. time.
2. With the axes parallel, position the field data curve over the type curve until field data match the line source solution.
3. Read a "match point" as the corresponding coordinates of any point common to both graphs, while aligned.
4. From the pressure and time match determine the values of two reservoir parameters, e.g., permeability (or permeability thickness) and porosity (or porosity thickness).

Additional phenomena and techniques discussed in the report include:

1. Skin effect--the additional pressure drop caused by the restriction of flow near the well.
2. Wellbore storage--a materials balance effect of fluids in the wellbore.
3. Analysis of bounded reservoirs.
4. Pressure drawdown test--a series of bottom-hole pressure measurements made during a period of constant producing rate flow; the skin effect, s, and the permeability, k, or the permeability thickness, kh, can be calculated.
5. Pressure buildup test--a graphical technique (possibly the most useful of all analyses) to obtain permeability, skin effect, and static average pressure.
6. Single and two-phase flow considerations.
7. Fractured wells.
8. Mass-energy balance method.

c. Physical Modelling

Work on the physical model was confined to administrative inquiries on the availability of hardware and costs for:

1. The model itself (see previous quarterly reports),
2. heating system, and
3. pressure/flow/temperature measurement instruments.

A decision was made to construct an unpressurized tank at first to test convection patterns. A more detailed treatment will be presented in the next quarterly report.

C. Future Work

1. Numerical Modelling of Geothermal Reservoirs

During the next quarter, numerical solutions for the problems of steady pumping and reinjection in a hot-water reservoir and the dynamics of the Ghyben-Herzberg lens will be initiated. The finite element solution of free convection in a geothermal reservoir with irregular geometry will also be formulated during the next three months.

2. Well Test Analysis and Physical Modelling

Emphasis during the coming quarter will be placed on three pursuits: 1) ordering parts and constructing the physical model; 2) coordinating with the Geophysical Drilling Program on well testing and hardware, and 3) developing the software associated with well test analysis.

Previous Hawaii Geothermal Project Engineering Program quarterly reports and Technical Reports No. 1 and No. 3 [1, 2] detailed the background information related to pursuit "1" and portions of "2" above. Some preliminary thoughts will therefore be outlined here for "2" and "3".

A comprehensive test program will be designed to suit allowed conditions. The quality and accuracy of performance prediction increase with longer measurement periods and equipment sophistication. A series of pressure drawdown and buildup tests will be scheduled to maximize information with respect to cost and time.

A set of computer programs will be developed incorporating the reservoir engineering techniques of the petroleum industry and the general materials/energy balance equations. In short, given the data from the well measurement program, that is, pressure, temperature and flow change with time, a computer will be utilized for performance matching purposes to obtain desired conditions, such as interference, reservoir volume, and initial pressure. A sub-program can then be used to predict optimal flow rates, total energy available, size of reservoir, and the like.

A subsequent software package considering the non-isothermal case will probably be initiated during the next quarter. The approach will be somewhat similar to the total systems petroleum reservoir engineering model.

D. References

1. Cheng, P. and Lau, K. H., "Steady State Free Convection in an Unconfined Geothermal Reservoir," Hawaii Geothermal Project Engineering Program, Technical Report No. 2, University of Hawaii, March 1, 1974. To appear in the *Journal of Geophysical Research*.

2. Takahashi, P., Chen, B., and Mashima, K., "Geothermal Reservoir Engineering: State-of-the-Art," Hawaii Geothermal Project Engineering Program, Technical Report No. 3, University of Hawaii, May 1, 1974.

3. Chen, B., "Geothermal Reservoir and Well Test Analysis: A Literature Survey," Hawaii Geothermal Project Engineering Program, Technical Memorandum No. 2, University of Hawaii, September, 1974.

TASK 3.6 OPTIMAL GEOTHERMAL PLANT DESIGN

Investigators: H. C. Chai, J. Chou, and D. Kihara

A. Timetable

December 31, 1974	1. Survey availability of components to be used with each working fluid 2. Construct components and assemble experimental heat transfer loop
June 30, 1975	1. Establish general requirements, ground rules, and design criteria for a research-oriented plant for liquid-dominated fields 2. Construct and test horizontal heat exchanger
December 31, 1975	1. Set up procedures for the design and selection of the components of regenerative binary fluid plants 2. Continue testing of horizontal heat exchanger and write computer program for horizontal heat exchanger 3. Begin testing of vertical heat exchanger
June 30, 1976	1. Lay out detailed flow diagrams of the plant based on a regenerative binary fluid system, with a vapor flashing system as the alternative 2. Analyze test data for horizontal heat exchanger and continue testing of vertical heat exchanger
December 31, 1976	1. Estimate capital costs of the plant, evaluate unit operating cost, and compare feasibilities of the two systems 2. Complete testing and analyze test data for vertical heat exchanger

B. Progress to Date

During the past quarter, work has been focused on five areas:

1. Thermodynamic properties of brine.
2. Deposition of calcite in wall casings--some methods of prevention.
3. Vapor flashing plant--a study of the characteristics of major components and system behavior.
4. Binary fluid cycle--the variety of possible working fluids extended.
5. Heat exchanger design--a parametric study of a vertical heat exchanger and set-up of experimental heat transfer loop.

1. Thermodynamic Properties of Brine

An accurate analysis of a geothermal energy system requires that the thermodynamic properties of the geothermal fluids in the system be available for use in the calculations. Unfortunately, the composition of geothermal fluids varies from well to well in a wide range; and even though the composition of a brine may be accurately determined by chemical analysis, only a few of the thermodynamic properties of brine have been measured and reported in the literature. Harned and Owen [1] and Robinson and Stokes [2] have reviewed the data and the theory for mixed salt solution. Previously reported experimental data are confined within the temperature limits of 100°C. In dealing with solutions, fugacity and activity coefficients are used in place of Gibbs free energy, as introduced first by Lewis and Randall. At a given pressure, the values of activity coefficient vary with temperature and composition, and are determined basically from measurements of electromotive force in the solution, distribution of a solute between two solvents, or vapor pressure. Theoretically, the other thermodynamic properties of a real solution can be evaluated from activity coefficients of its components. Any extensive property of a solution may be found by summing the product of the moles of each component times its partial molal property. For the enthalpy and volume of an ideal solution, the partial molal value of a given component is equal to the specific property of the component in pure state at the same pressure and temperature. The deviations of the values of enthalpy and volume of a real solution with i components from those of an ideal solution can be expressed in terms of activity coefficient a_i:

$$H - \Sigma_i n_i h_i = -RT^2 \Sigma_i n_i \frac{\partial}{\partial T} \ln a_i$$

$$V - \Sigma_i n_i v_i = +RT \Sigma_i n_i \frac{\partial}{\partial p} \ln a_i$$

Since the calculations involve the partial derivatives of the logarithm, extremely accurate values of a_i are required for obtaining significant results. Because very precise measurement for the activity coefficient is difficult, the accurate data in publications are limited to a few binary or ternary solutions in a narrow range of temperatures and pressures, and they are insufficient for determining the properties of geothermal fluids.

Under the sponsorship of the Office of Saline Water, many investigations have been done to provide basic data on thermodynamic properties of sea water and brackish waters encountered in desalination processes. Fabuss and Korosi [3] measured densities and vapor pressures of binary and ternary solutions containing NaCl, KCl, Na_2SO_4 and $MgSO_4$ in the temperature range of 25°C to 175°C at low pressures for concentrations up to a concentration factor of five times the normal concentration of sea water. Based on their experimental data, the correlation techniques and equations were developed for the brackish water solutions. Heat capacities of NaCl, KCl, $MgSO_4$ and $MgCl_2$ solutions and sea water have been carefully measured at temperatures up to 400°F for concentrations up to 120 ppt by Bromley [4], who also measured the heats of mixing of sea salt solutions to determine the values of enthalpy. Liu and Lindsay [5] made precise measurements on a solution which has an ionic composition to simulate sea water at concentration factors of 1.5 to 10 for temperatures of 75°C to 300°C, and they calculated the activity coefficients and excess partial molal properties.

The real nature of solutions has yet to be discovered. The Debye-Hückel theory only explains the behavior of strong electrolytes in very dilute solutions; for solutions with salts higher than 0.1 mole per 1,000 grams of solvent, several modified versions of the equation have been proposed to fit the experimental data and, as a rule, extra terms are added to the basic equation without theoretical justification. In reality, all the modified equations are empirical equations. An equation which adequately represents the property relations, even if it is empirical, can be used to interpolate experimental data, to facilitate calculations, and to provide a concise representation of a large mass of data. An efficient evaluation of the properties

is impossible without interpolation formulae. Based on the data in the literature, Chou [6] formulated the interpolation formulae for vapor pressures, specific volumes, enthalpies, and heats of vaporization of ordinary sea water in the temperature range of 0°C to 200°C for salinities of 0 to 120 ppt. Since sea water is only slightly compressible, the difference of properties between sea water at vapor pressure and sea water at a higher pressure at the same temperature is negligible if the pressure is only 100 psi or so higher than the vapor pressure. In such a case, the recommended formulae for vapor pressure, heat of vaporization, specific volume, and enthalpy are as follows:

Vapor pressure,

$$\ln p = (1 + ax + bx^{1.5}) \ln p_w + (cx + dx^{1.5} + ex^2)$$

$$\ln p_w = 71.023834 - 7380.4001/T - 9.0977349 \ln T + 0.0070871862T$$

$$a = 0.36403381 \times 10^{-5} \qquad b = -0.21880179 \times 10^{-5}$$

$$c = -0.89742462 \times 10^{-3} \qquad d = 0.44991149 \times 10^{-5}$$

$$e = -0.54721135 \times 10^{-5}$$

where T is the temperature in degrees Kelvin. p is the vapor pressure of sea water in bars in the temperature range of 20°C to 150°C for chlorinities x ranging from 0 to 70 ppt. The term chlorinity is internationally defined as parts of equivalent chloride per thousand parts of sea water, and the ratio of salinity to chlorinity is close to 1.811. The ratio of total salt content to salinity is about 1.0046.

Heat of vaporization,

$$h_{fg} = 854.52547 - 1.5939341T + 0.34368756 \times 10^{-2}T^2 - 0.38341991 \times 10^{-5}T^3$$

$$+ T(0.92968267 \times 10^{-4}S - 0.1282345 \times 10^{-4}S^{1.5} + 0.195061 \times 10^{-5}S^2)$$

$$- (0.77803108 \times 10^{-2}S + 0.75123967 \times 10^{-3}S^{1.5} + 0.38753341 \times 10^{-3}S^2)$$

where S is the salinity in ppt, T is the temperature in degrees Kelvin, and h_{fg} is the heat of vaporization of water in calories per gram.

Specific volume,

$$v = 5.5839889 - 0.0096615179T + 0.8724311 \times 10^{-5}T^2 - 1057.246/T + 95122.242/T^2 - x(0.0063811748 - 0.31038891 \times 10^{-4}T + 0.47689449 \times 10^{-7}T^2) + x^2(0.53558009 \times 10^{-4} - 0.31012679 \times 10^{-6}T + 0.45483252 \times 10^{-9}T^2)$$

where v is the specific volume of sea water in cubic centimeters per gram in the temperature range of 20°C to 150°C and the concentration range of 5 to 70 ppt chlorinity, T is the temperature in degrees Kelvin, and x is the chlorinity.

Enthalpy,

$$h = h_{298.15°K} + \int_{298.15°K} C_p dT$$

$$h_{298.15°K} = 25.035(1-w) - wq_d$$

$$q_d = -37.991497w^{0.5} + 182.6251w - 208.77039w^{1.5} + 40.503419w^2$$

$$C_p = A + BT + CT^2 + D/T + (E + FT + GT^2 + H/T)S + (I + JT + KT^2 + L/T)S^2$$

$A = 1.3958222$ $\quad B = -0.23878998 \times 10^{-2}$

$C = 0.36362594 \times 10^{-5}$ $\quad D = -2.3078127$

$E = -0.70418481 \times 10^{-3}$ $\quad F = 0.78180236 \times 10^{-5}$

$G = -0.1626327 \times 10^{-7}$ $\quad H = -0.43916216$

$I = -0.44503885 \times 10^{-5}$ $\quad J = -0.14563778 \times 10^{-7}$

$K = 0.40243346 \times 10^{-10}$ $\quad L = 0.20799146 \times 10^{-2}$

where h is the enthalpy of sea water in calories per gram over a range of temperatures from 0°C to 200°C, and of concentrations from 10 to 120 ppt, T is the temperature in degrees Kelvin, w is the weight fraction of the salts, and S is the salinity in ppt. The values of enthalpy calculated by the above equation are based on the standard state of zero enthalpy for salts in sea water at infinite dilution at 25°C.

In general, geothermal brines are electrolyte solutions containing high concentrations of sodium and chloride ions. Since it is not possible to measure the exact thermodynamic properties of a particular type of brine, the properties of pure water are usually used as an approximation in geothermal engineering calculations. To improve the degree of exactness, the properties of sea water at an equal ionic strength or total solid content can be applied to the calculations.

2. Deposition of Calcite in Well Casings

Precipitation of calcite occurs inside a well from the top down to a depth where the upset of $CaCO_3$-CO_2-H_2O equilibrium begins. A loss of 1 ppm calcium ions from the brine which emerges from a typical well at 1/2 million pounds per hour can amount to 1 pound of $CaCO_3$ deposit per hour, and in two months the deposit can fill a 24-ft. length of 8-in. diameter hole. The fluid through the well is not in chemical equilibrium. The rate of precipitation is affected by the concentration of carbon dioxide in the vapor. Morse [12] studied the reaction kinetics of calcium carbonate in sea water to find out that the time of complete dissolution of calcite can be from a few minutes to several hours depending upon the change of the pH of the solution and the partial pressure of carbon dioxide. The deposit in the well may be eliminated or reduced by throttling the valve at wellhead to increase the partial pressure of carbon dioxide, but such a measure results in a reduction of the flow rate.

The deposit may be allowed for a limited period of time if it can be removed periodically. The most frequent method of removing the inside scale of a tube is to use a revolving tool to scrape the scale off; however, the mechanical removal of deposit in a well casing, although often practiced, is not satisfactory because the falling of the cutting chips may plug the well screen and fill up the lower section of the well. It might be a good idea to design a mechanical cleaner which can pulverize the deposit and dispose of the fine chips with a vacuum cleaner. Another method of removing the scale is a chemical treatment. A rapid deposit of calcite has occurred in some wells in Hungary at a depth of 30m to 50m, Belteky reported [7]. The experiments with hydrochloric acid were found very successful there. Corrosion due to the acid was controlled by adding an inhibiting agent. It was possible to time the acid treatment without any halt in production. The depth for the addition of acid was determined in accordance with the formation of scale.

When the hot brine flows through the well by natural forces, the pressure exerted on the fluid decreases due to the change of potential energy and friction. The water vapor flashes out as the pressure is lowered to the vapor pressure corresponding to its temperature. If the partial pressure of carbon dioxide in the vapor phase is not enough to prevent the evolution of gaseous carbon dioxide from the solution, the carbonate ions react with calcium to form calcite deposits. A method being considered by some engineers is to pump the the brine out by a submersible pump to prevent the formation of calcite deposits. The well casing is sealed at the top, and the brine is delivered through a concentric discharge pipe. Thus, no gaseous carbon dioxide can be evolved in the well. However, the construction of a pump to handle hot corrosive fluid in a deep well is technically very difficult. The projected capital cost and the life of a pump also discourages engineers from adopting this method, at least for the time being.

Another method of solving the calcite problem is to inject compressed carbon dioxide into the well. This principle has been suggested by Rogers Engineering Company [13]. A possible scheme is shown in Fig. 3.6-1 for a vapor flashing plant. One of the major concerns is the compressor power required. To maintain 0.2 atmosphere partial pressure of carbon dioxide at a total wellhead pressure of 100 psia, the rate of gas reinjection is about 7,400 pounds per hour for a steam flow at 100,000 pounds per hour. The power required to compress 7,400 pounds of carbon dioxide in the exhaust condition of 2 psia and 120°F to 300 psia pressure is 950 horsepower, assuming a compressor efficiency of 70%. Obviously, the economical justification of this scheme depends upon the required amount of carbon dioxide to be recycled.

A dilute solution behaves as an ideal solution in which the solvent obeys Raoult's law and the solute satisfies Henry's law, which states that the mole fraction x_i of a gas dissolved in a very dilute solution, at constant temperature, is proportional to the partial vapor pressure P_i of the gas.

$$x_i = P_i/K$$

where K is an empirical constant which depends solely upon the temperature and the nature of the solvent. Malinin [11] and Ellis and Golding [10] measured the solubility of carbon dixoide in the temperature range of 50°C to 300°C. The values of the constant K for the solution of carbon dioxide in water and sodium chloride, determined by Ellis and Golding, were fit into an equation by the least square method as follows:

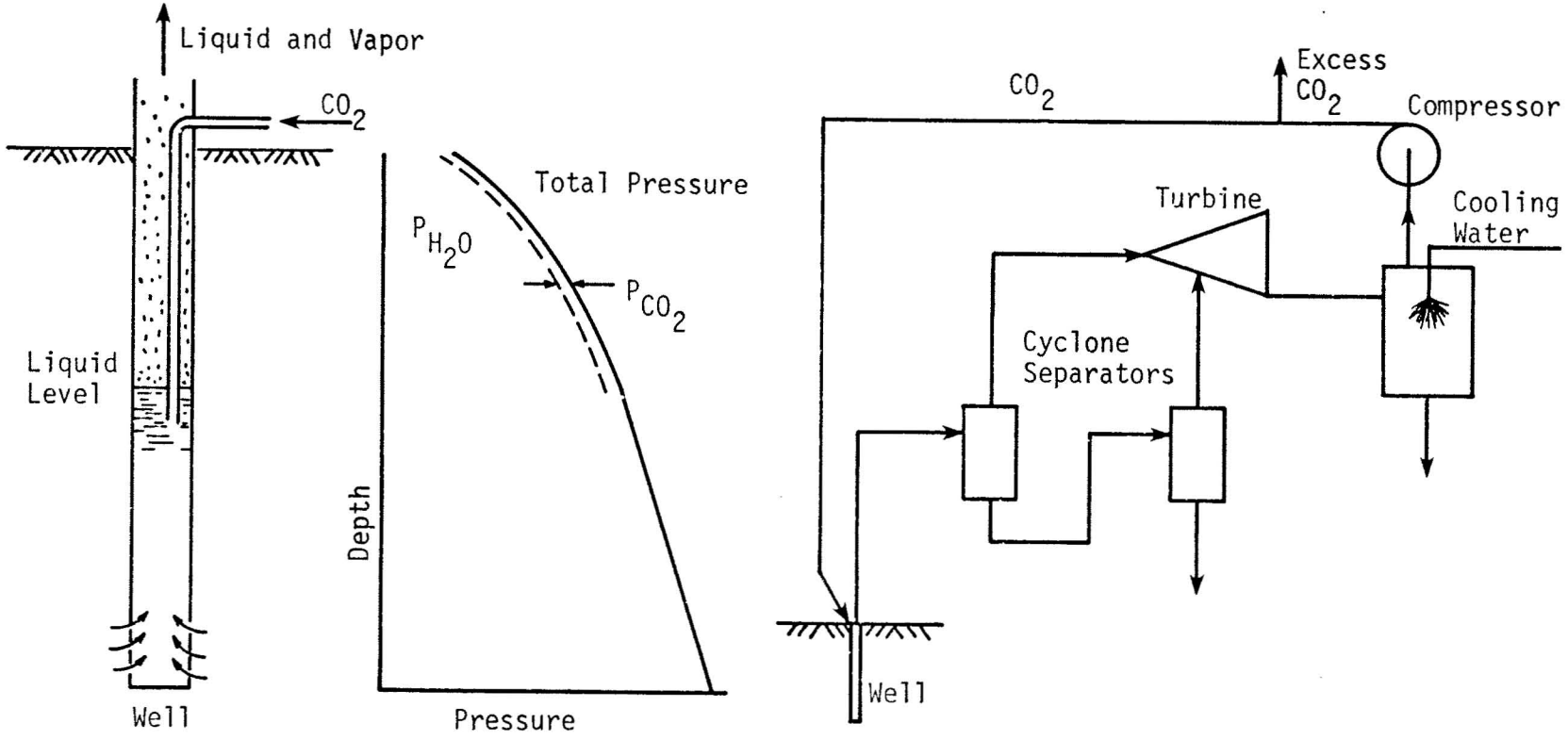

FIG. 3.6-1 REINJECTION OF CO_2 INTO WELL

$$K = 1212 + 1201.6m - 465m^2 + (99.6 - 8.05m + 11.84m^2)t$$
$$+(-0.39 + 0.08m - 0.075m^2)t^2 + (0.3846 - 0.151m + 0.139m^2)t^3$$

where m is the molality of sodium chloride, t is the temperature in degrees centigrade, and the unit of partial pressure of carbon dioxide is atmosphere. The standard error of estimate of K is in the order of 400. As the degree of accuracy of curve fitting is limited by the consistency of data points, the above equation is sufficiently accurate for the available data. The dependence of solubility of carbon dioxide on temperature is illustrated in Fig. 3.6-2 for water and an aqueous sodium chloride solution of 1m concentration.

When calcite (calcium carbonate) is placed in water which is open to gaseous carbon dioxide, the calcium and bicarbonate ions exist in the solution. Ellis [8, 9] measured the solubility of the calcite in water and in sodium chloride solutions. At partial pressures up to about 60 atmospheres and temperatures up to 300°C, the solubility of calcite varies as the cubic root of the partial pressure of carbon dioxide. Since the pressure dependence of the partial molal volume of a component in the solution is small, the change of its activity is negligible if the change of pressure is only 20 or 30 atmospheres. By using the mean activity coefficients determined by Ellis in terms of ionic strength at 12 atmospheres of P_{CO_2}, the solubility of calcite in a sodium chloride solution at other pressures can be estimated. The ionic strength is equal to the molality of NaCl plus 3 times the molality of $Ca(HCO_3)_2$. Fig. 3.6-3 illustrates the relationship of calcite solubility, concentration of NaCl, and temperature at P_{CO_2} of 5 and 20 atmospheres when the system is in chemical equilibrium.

In a liquid-dominated field, there might be a vapor space which can be located by geophysical survey. If so, by drilling a well to vent the carbon dioxide out, the calcium ions can be removed from the reservoir, and the well casing will be free from calcite deposits. During the venting, steam comes out with the non-condensable gases; a portable non-condensing plant may be used to utilize the energy in the transient period. In principle, it would be most desirable to lower the concentration of calcium ions by relieving the partial pressure of underground carbon dioxide. The suggestion of venting the underground carbon dioxide out deserves careful consideration if the deposition of calcite in the well casing is a serious problem.

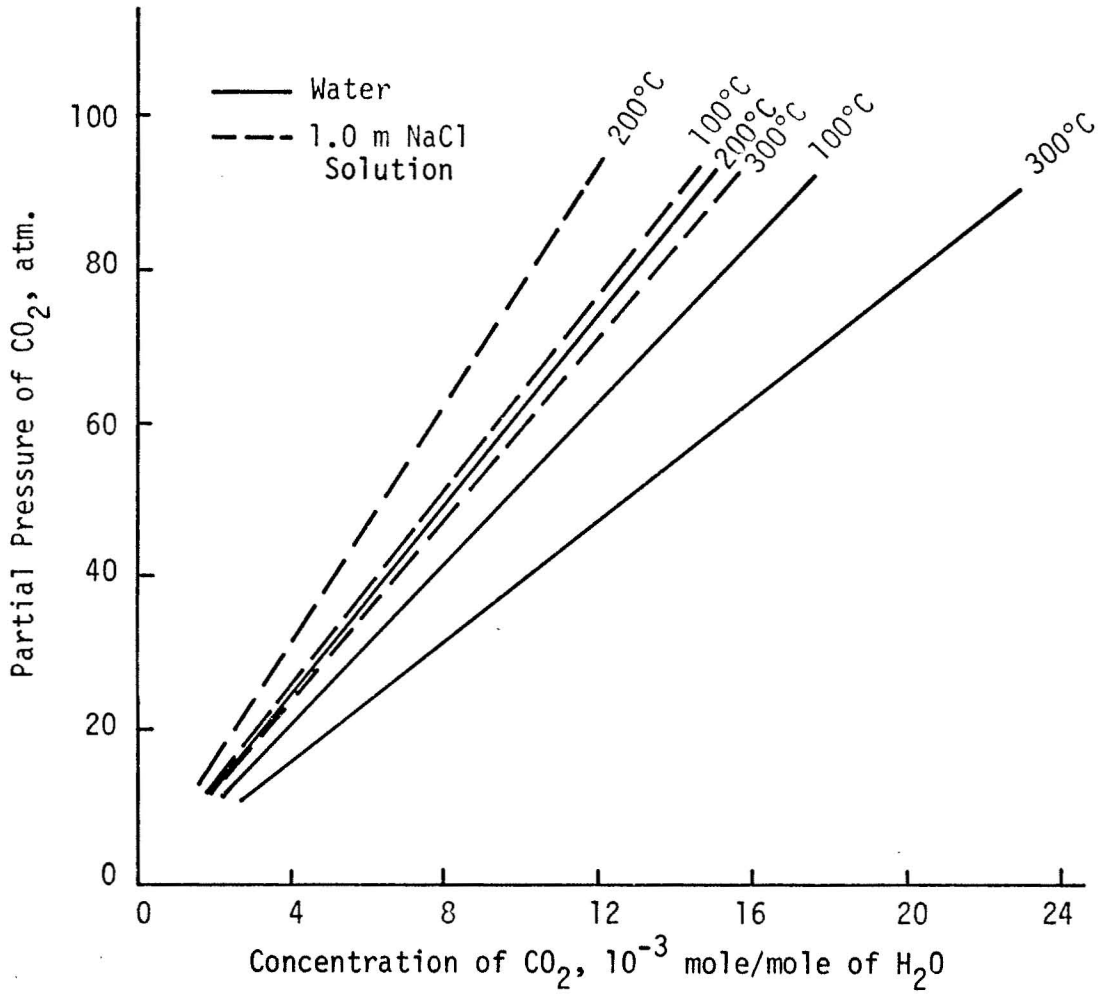

FIG. 3.6-2 DEPENDENCE OF SOLUBILITY OF CO_2 ON TEMPERATURE AND NaCl CONCENTRATION

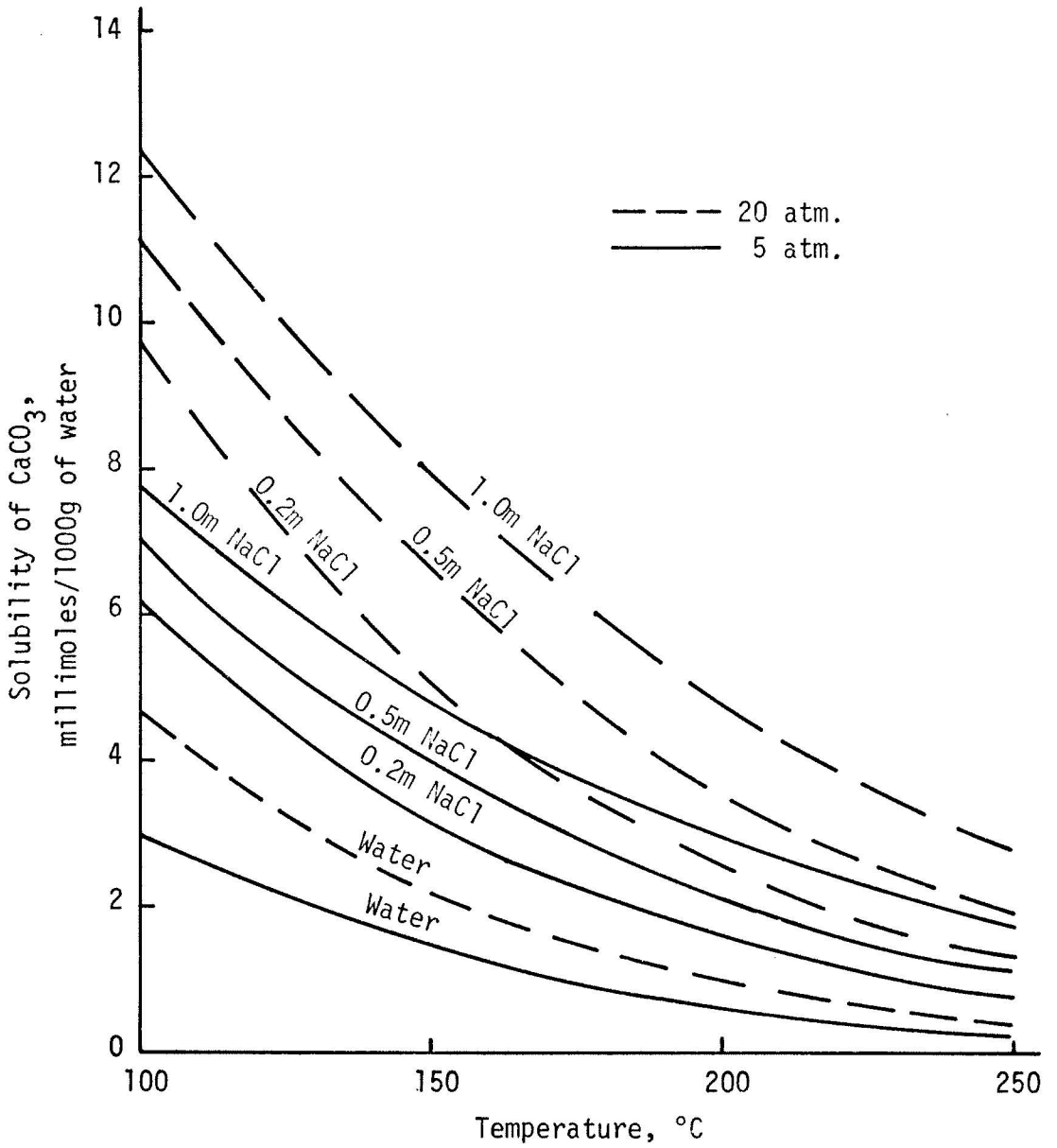

FIG. 3.6-3 SOLUBILITY OF CALCITE IN SODIUM-CHLORIDE SOLUTIONS AT 5 AND 20 atm. PARTIAL PRESSURE OF CO_2

3. Vapor Flashing Plant

The characteristics of major components and the system behaviors of vapor flashing plants have been studied from the information being reported in publications. The power output increases with the number of flashing stages. For obtaining the maximum power, approximately the optimum flashing pressures correspond to the saturation temperatures which are equally divided between the saturation temperature of hot water to the plant and the condensing temperature. For economical reasons, the number of flashing stages is generally limited to two. For a typical well, the flow rate decreases as the wellhead pressure increases. The optimum wellhead pressure varies with reservoir conditions and plant arrangement, and it is around 100 psig in most cases.

To maintain a high vacuum in a condenser, the non-condensable gases must be removed continuously from the condenser. When the non-condensable gas content is low, a steam jet ejector should be used because of its simplicity and reliability. For removing a large quantity of non-condensable gases, a centrifugal vacuum pump is recommended in consideration of the energy savings. The condensing pressure affects the capital cost of the plant and the unit cost of power produced. The lower the condensing pressure, the lower the steam rate of the turbine; however, the accessory power required by gas-removing equipment, circulating water pump, condensate pump, and cooling tower fan increases as the condensing pressure decreases. The optimum condensing temperature has to be determined by heat balances and cost analyses. The higher the gas content in the exhaust, the higher the optimum condensing pressure. In general, the condensing pressure of a geothermal plant is much higher than that of a conventional power plant. In the existing geothermal plants, the condensing pressures at design conditions vary from 2 to 4 in. Hg. abs.

The condensers are of a direct-contact type since recycling of the condensate is not required. If a barometric condenser is used, it is very desirable to locate the plant in a site where the tailpipe of the condenser can be easily installed without much complication of the plant arrangement. If an adequate amount of cooling water from a natural source is not available, a cooling tower must be used to recycle the cooling water. The cooling tower can be either a dry or wet type. The dry towers are not suitable for a geothermal plant. The draft of a wet cooling tower can be produced mechanically or naturally, and the natural draft towers are not economical for plants having

ratings of less than 150 MW. The induced-draft, cross-flow type of tower has distinct advantages over other types because the distance of air travel and the height of the fill can be adjusted to minimize the loss of draft. The cooling tower theory is well known, and the methods are available for estimating the performance and the dimensions.

The turbine is the most expensive and the most critical component in the plant. There is no standard for turbines in geothermal plants. Every turbine must be specially designed to suit the chemical quality of the steam and other operating conditions. Although the exact performance of a turbine is not known until the bidding from manufacturers is received, there is sufficient information from the publications to estimate the steam rates in terms of the size, loading, throttle pressure, inlet temperature, and condensing temperature.

The cyclone separators are used to separate the steam out from the mixture of steam and water, or to flash out the steam from the hot brine by lowering the vapor pressure. The bottom-outlet-cyclone separator has been successfully adopted in New Zealand. It is capable of producing steam at a quality of 99.9 per cent or better.

The mixture of steam and water can be transported in a single pipe without the problem of water hammer, cavitation, and vibration. The pressure drop of a two-phase flow may be determined by the Lockhart and Martinelli correlation. Both the thermal efficiency and the cost of a plant can be improved by transporting the mixture in a single pipe instead of using one pipe for steam and another for water.

A great deal of experience in the design and operation of vapor flashing plants has been accumulated in New Zealand, Japan, and Mexico. The economic feasibility of producing power by flashing steam has long been established, and vapor flashing plants may dominate the geothermal power production in liquid-dominated fields continuously for years.

4. Binary Fluid Cycle

The list of possible working fluids that may be used in a simple Rankine cycle was extended to include additional substances with a wide range of properties. The fluids considered and their relevant characteristics are given in Table 3.6-1.

The analysis of the power producing cycle was conducted for the following set of conditions:

TABLE 3.6-1 WORKING FLUIDS AND PROPERTIES

Fluid	Critical Point		Boiling temp. at atm press.	Liquid density at 100°F	Vapor spec. vol. at 100°F
	T_c °F	p_c psia	T_{sat} °F	ρ_f, lbm/ft^3	v_g ft^3/lbm
R-11 CCl_3F	338.4	640.0	74.9	90.21	1.765
R-113 CCl_2-$CClF_2$	417.4	498.9	117.6	95.79	2.976
R-114 $C_2Cl_2F_4$	294.3	473.0	38.8	88.40	0.696
R-C318 C_4F_4	239.6	403.6	21.5	90.33	0.382

Net power output	10 MW
Condenser outlet conditions	Saturated liquid at 100°F
Heat source	Liquid brine at temperature indicated
Turbine efficiency	85%
Pump efficiency	75%
Pinch point temperature difference	20°F
Pressure losses and heat losses neglected	

The results of the analysis can be viewed from two perspectives. If the cycle is considered by itself, i.e., independent of the heat source, then the thermal efficiency, given by η = Net work output/Gross heat input, would be one of the primary factors to be selected. The variation of this parameter as a function of the turbine inlet temperature, i.e., the maximum temperature that the working fluid experiences, is shown in Figs. 3.6-4 and 3.6-5. The performances of these four fluids are shown for various working pressures and for brine inlet temperatures of 325°F and 375°F. In almost all instances the curves are essentially flat indicating that the efficiency is relatively insensitive to turbine inlet temperature. In a few cases, the curves have negative slopes, viz., thermal efficiency decreasing as turbine inlet temperature increases. This is due to the fact that the fluid exiting the turbine has increasingly higher degrees of superheat which must be rejected in the condenser.

If the consumption of hot brine is to be the governing factor, Figs. 3.6-6 and 3.6-7 which show the required brine flow rate as a function of turbine inlet temperature are essential. Again, these figures are for brine temperatures of 325°F and 375°F.

There are some interesting observations to be made from Figs. 3.6-6 and 3.6-7. In general, all curves have positive slopes, which indicates that as turbine inlet temperature is increased, a greater flow rate of brine is required. This trend becomes more pronounced as the brine temperature increases.

Furthermore, by comparing the efficiency curves with the brine flow rate curves for the same brine temperature, it is seen that those working fluids which yield the highest efficiencies are not necessarily those which require the smallest brine flow rates.

The variation of required brine flow rate with brine inlet temperature is shown in Figs. 3.6-8 to 3.6-10. As would be expected, for a given power output, the higher the brine inlet temperature, the lower the flow rate required.

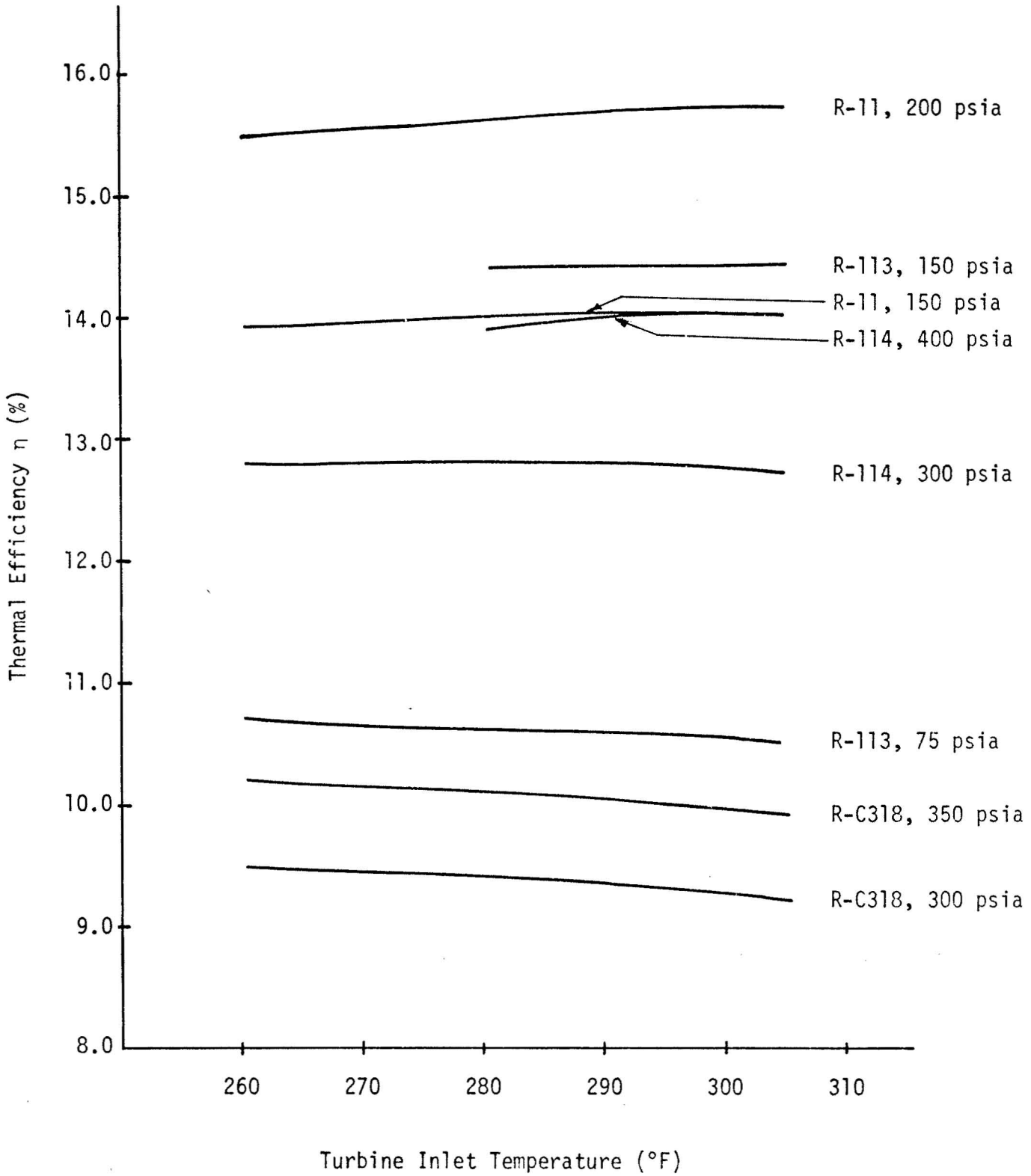

FIG. 3.6-4 THERMAL EFFICIENCIES USING VARIOUS WORKING FLUIDS WITH BRINE AT 325°F

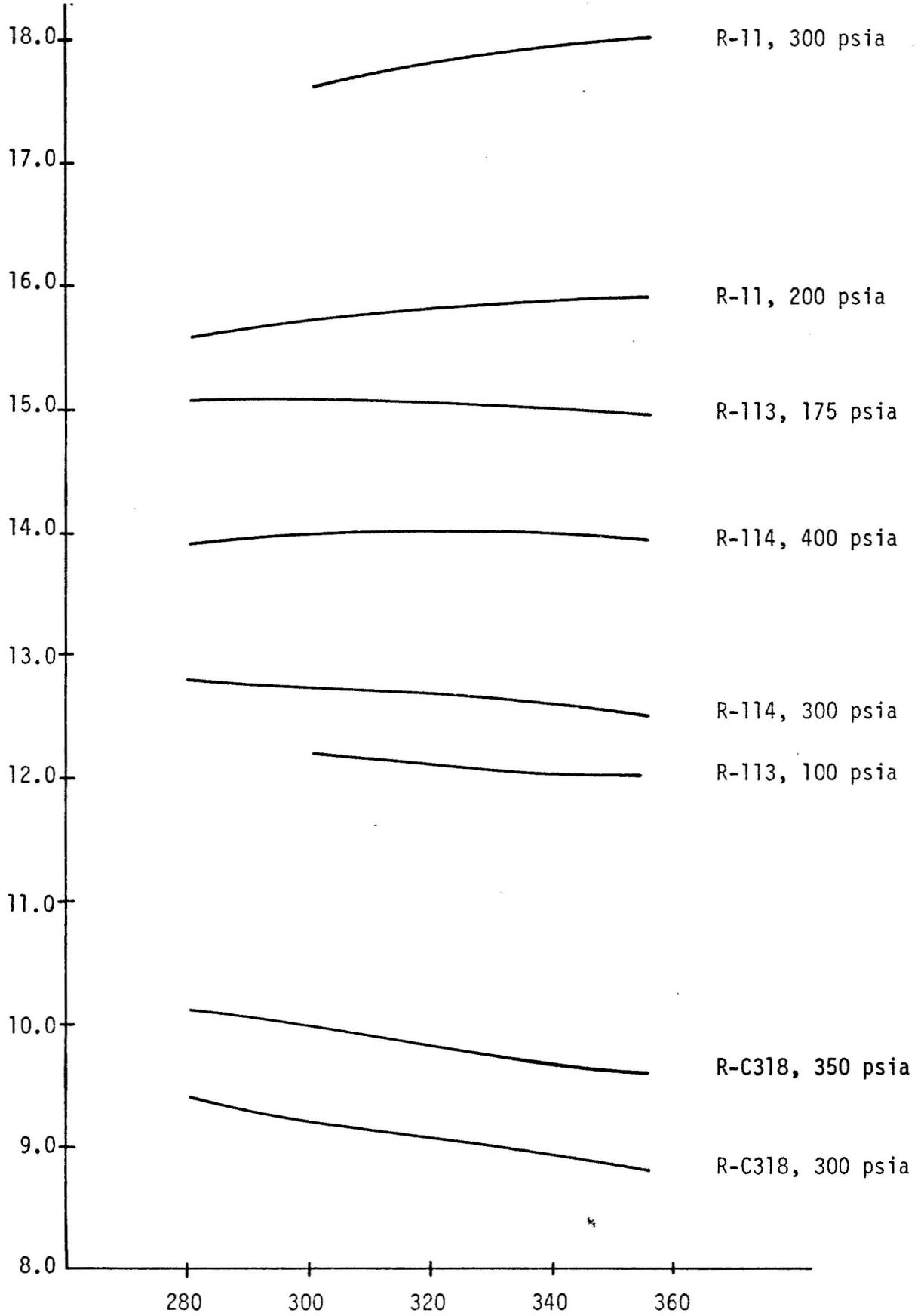

FIG. 3.6-5 THERMAL EFFICIENCIES USING VARIOUS WORKING FLUIDS WITH BRINE AT 375°F

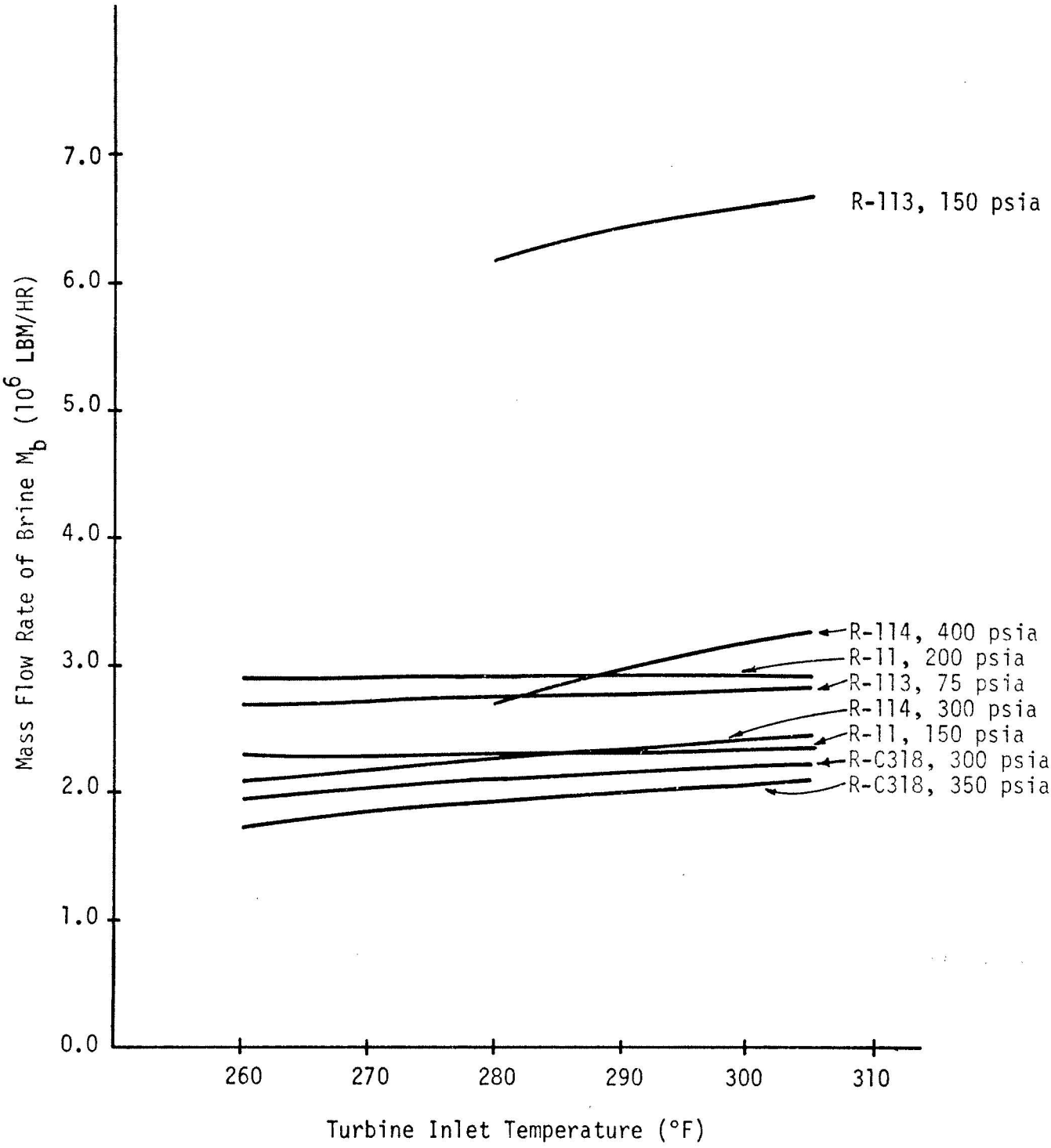

FIG. 3.6-6 BRINE FLOW RATES USING VARIOUS WORKING FLUIDS WITH BRINE AT 325°F

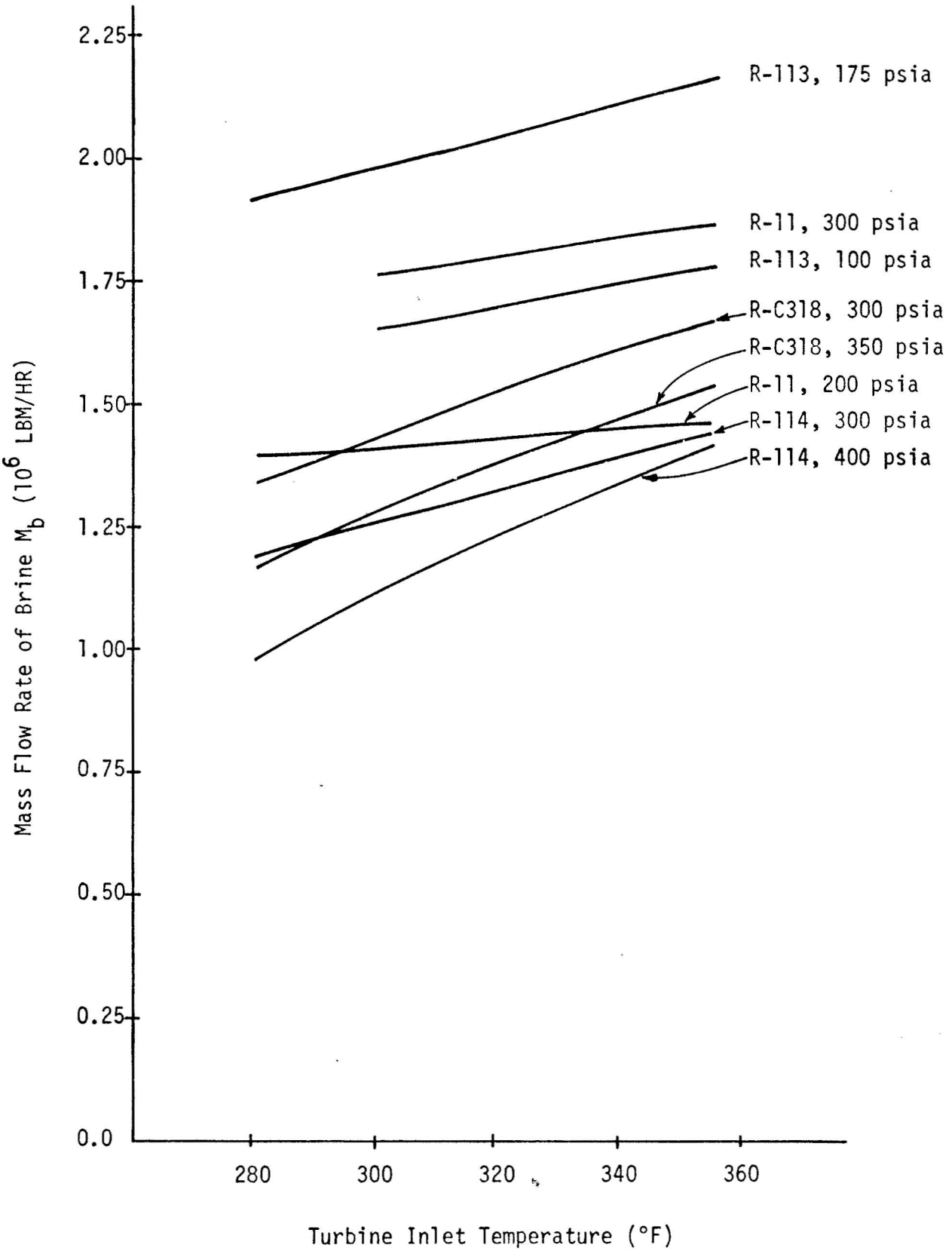

FIG. 3.6-7 BRINE FLOW RATES USING VARIOUS WORKING FLUIDS WITH BRINE AT 375°F

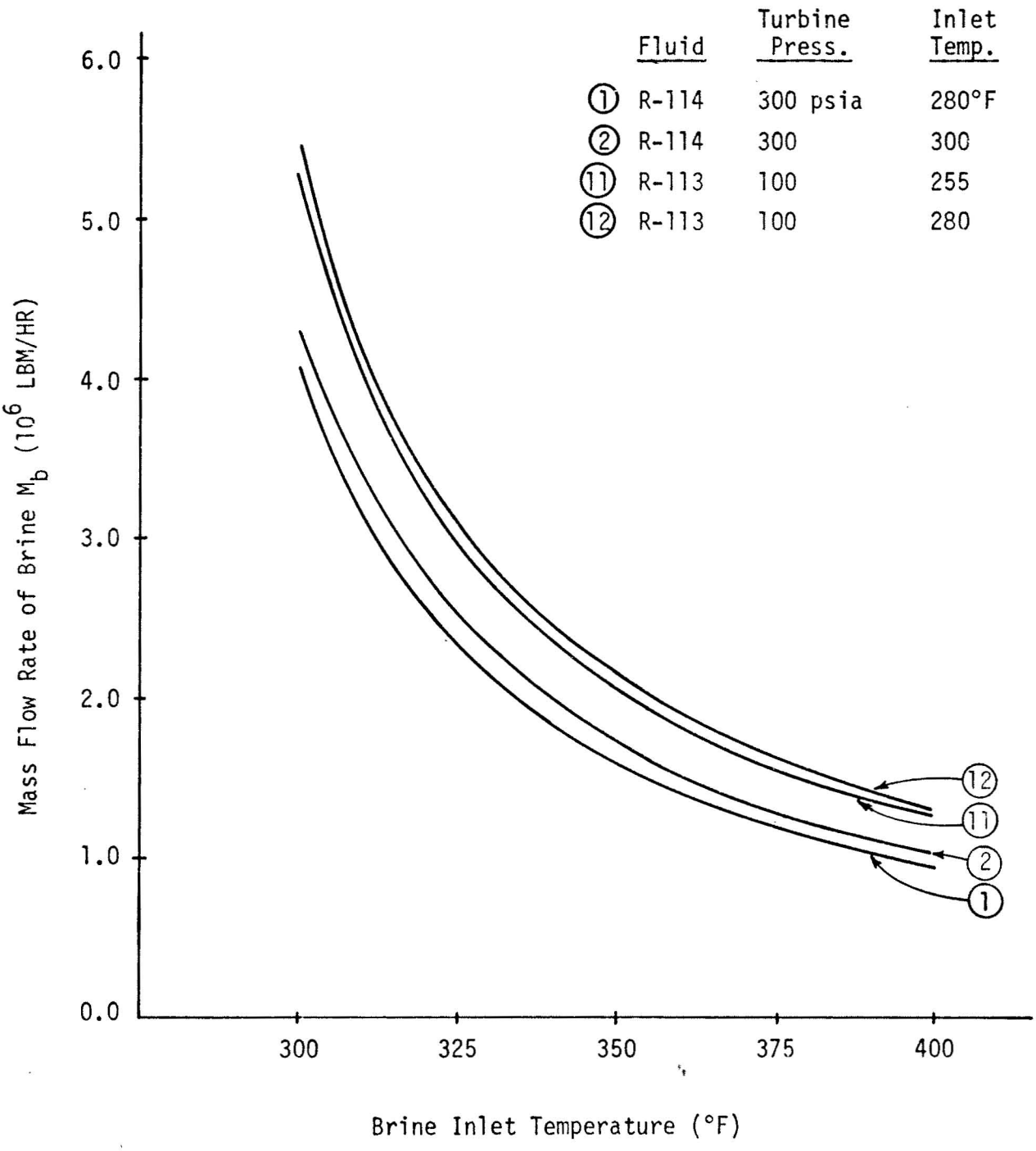

FIG. 3.6-8 BRINE FLOW RATES USING R-113 and R-114

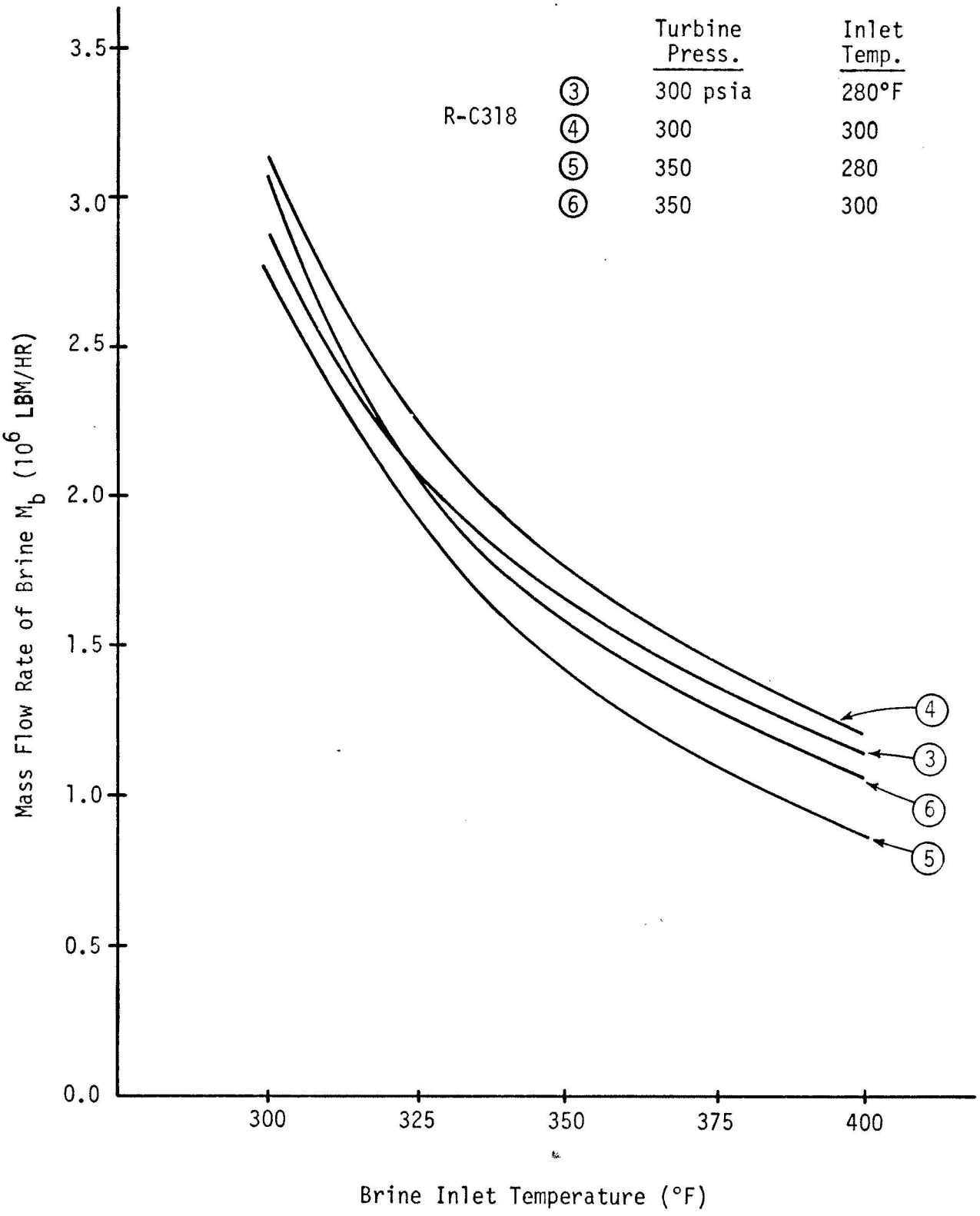

FIG. 3.6-9 BRINE FLOW RATES USING R-C318

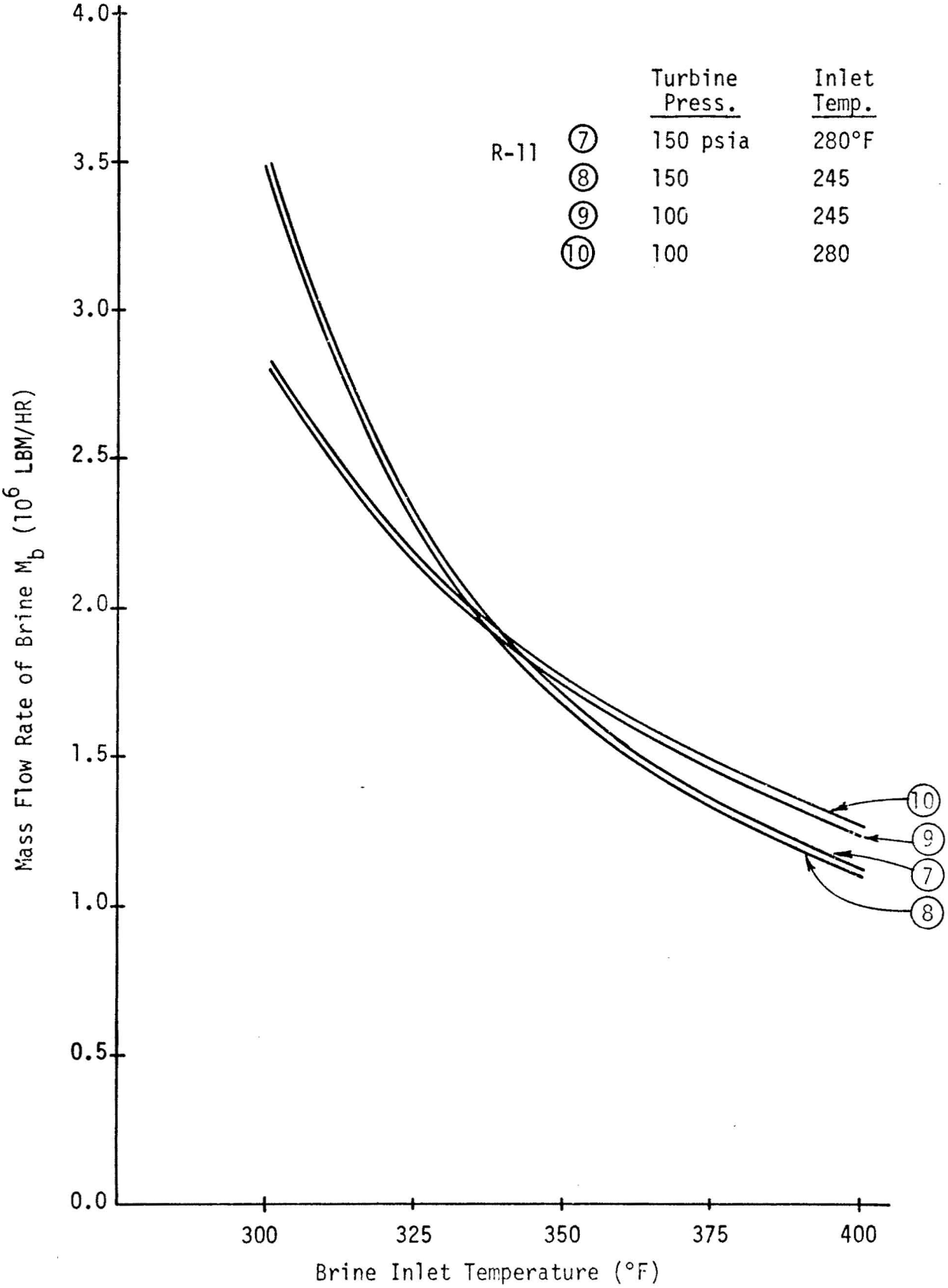

FIG. 3.6-10 BRINE FLOW RATES USING R-11

In scanning Fig. 3.6-10, it is seen that for brine inlet temperatures less than 335°F, the lower pressure, viz., 100 psia, requires the smaller flow rate, while for temperatures greater than 335°F, the higher pressure, 150 psia, requires the smaller flow rate.

5. Heat Exchanger Design

a. Parametric Study of a Vertical Counterflow Heat Exchanger

In previous quarters the design of a vertical counterflow heat exchanger, which was to be the prime heat exchange unit between the hot brine and the working fluid in the power producing cycle, was designed assuming the following standard set of conditions:

Heat source	Liquid brine at 350°F
Net power output	10 MW
Working fluid	R-600a - isobutane
Condenser outlet conditions	Saturated liquid at 100°F
Tube diameter	1 inch
Pitch	1.1
Isobutane velocity	7 ft/sec
Pinch point temperature difference	20°F
System pressure	400 psia
Scale thickness	Zero

Pressure losses and heat losses neglected

The details of a parametric study just concluded are detailed in a Technical Report being prepared. However, a summary of some of the results is presented here. In this parametric study, one parameter was varied while all of the others were kept constant. In this fashion significant trends could be more easily detected.

The variation of total length required as a function of turbine inlet temperature is shown in Fig. 3.6-11. This was part of the standard design but is shown here to give an indication of the lengths to be expected in a heat exchanger of this type. It is interesting that a minimum for the required tube length exists at a temperature of approximately 290°F.

In Fig. 3.6-12, the inside tube diameter is the parameter varied. As the diameter is decreased, the total tube length decreases but the number of tubes increases to compensate for the decrease in surface area per tube.

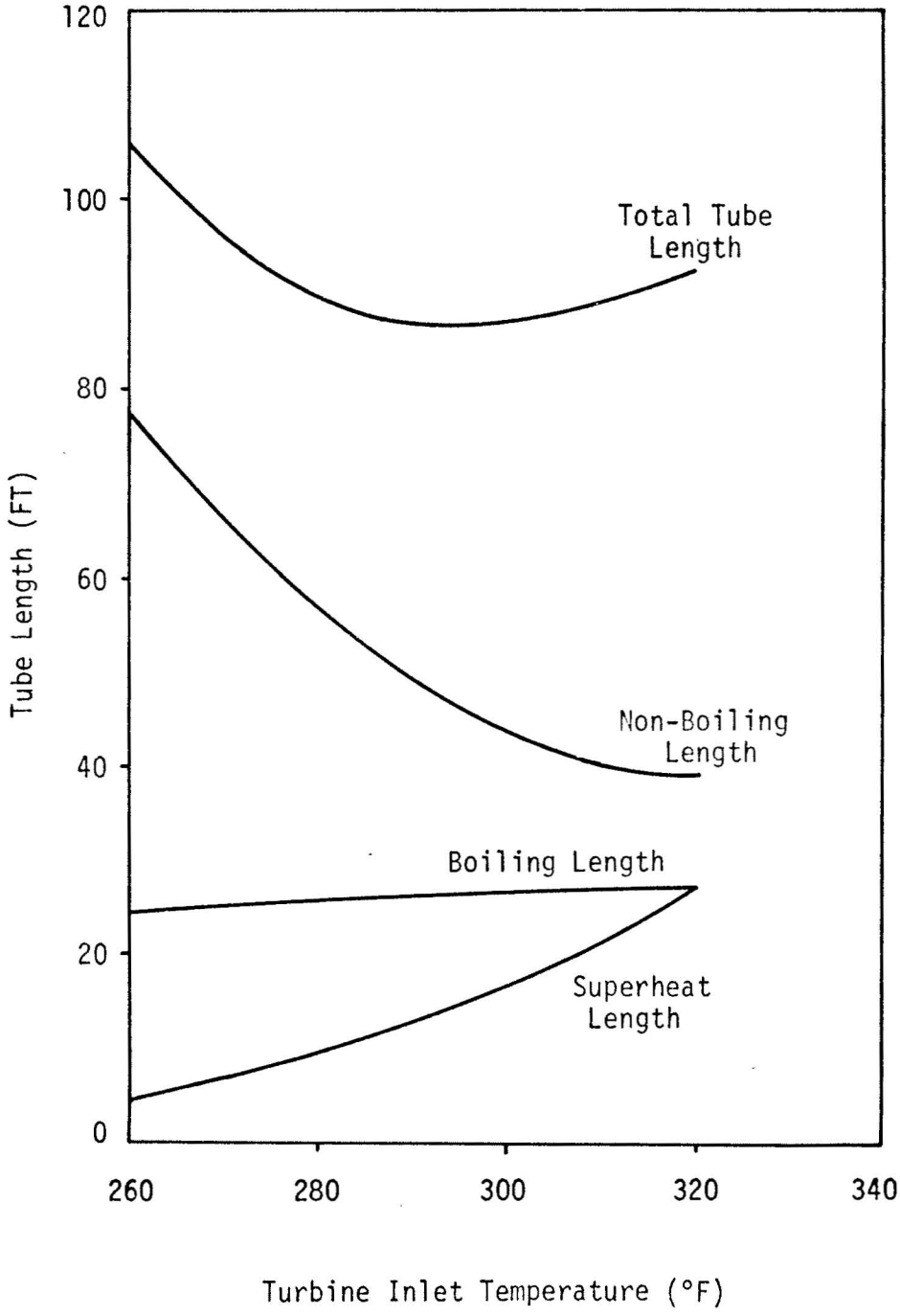

FIG. 3.6-11 THE EFFECT OF TURBINE INLET TEMPERATURE ON TUBE LENGTHS

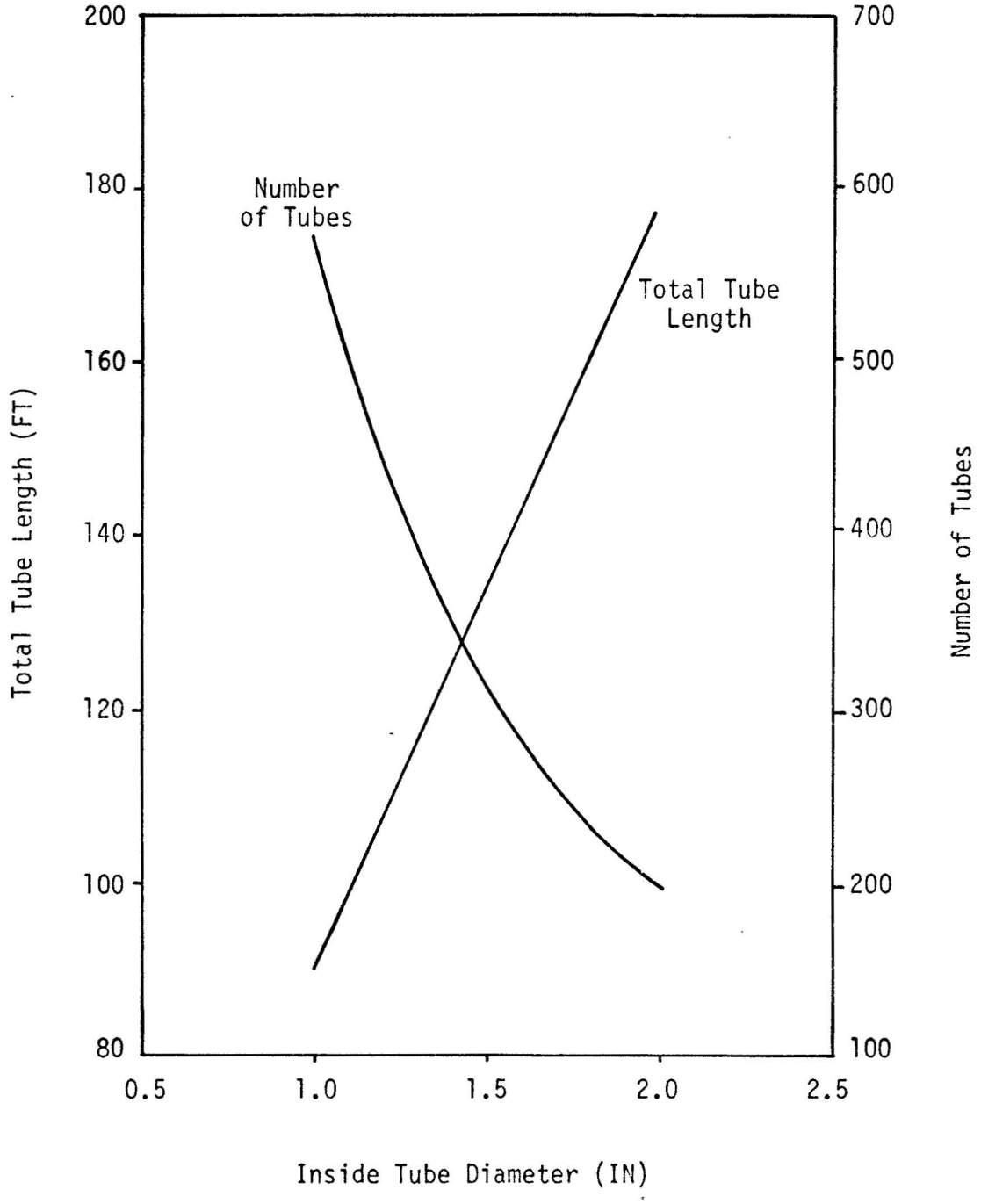

FIG. 3.6-12 THE EFFECT OF TUBE DIAMETER ON TUBE LENGTH AND NUMBER OF TUBES

Fig. 3.6-13 shows the variations of tube length and pressure drop with isobutane velocity. As both tube length and pressure increase markedly with isobutane velocity, there is good reason to keep the velocity of the working fluid at a fairly low value. Of course, a lower velocity means that the flow cross-sectional area must be increased in order to permit the mass flow rate of the working fluid to remain constant.

The pinch point temperature difference is another important parameter to be considered. The effect of this parameter on tube length, pressure drop, brine flow rate, and brine exit temperature is depicted in Figs. 3.6-14 and 3.6-15. It is seen that while a larger pinch point temperature difference is advantageous in terms of shorter tube length and smaller pressure drop, it results in a greater flow rate of brine required and a higher brine exit temperature.

Probably the overriding factor in the design of heat exchangers for geothermal power is that of scale deposition. Because of its low thermal conductivity and roughness, failure to prevent the deposition of scale can be disastrous. As seen in Fig. 3.6-16 the presence of 0.030 inch of scale on a 1-inch diameter is sufficient to cause a doubling of the tube length required and the resulting pressure drop.

The effect of tube pitch, the ratio of distance between tubes to tube diameter, on tube length and number of tubes is shown in Fig. 3.6-17. Here the two curves have slopes of opposite signs so that some sort of trade off must be decided upon.

b. Experimental Heat Transfer Loop

A test apparatus was designed to investigate the heat transfer and pressure drop characteristics of Freon-11 on the outside surfaces of a tube bundle. The schematic diagram of the test loop is shown in Fig. 3.6-18. The heat exchanger can be set up in either a horizontal or vertical configuration.

The purpose of this investigation is as follows:

Vertical Heat Exchanger

Compute the average heat transfer coefficient and the pressure drop from experimental data, and compare these results with those values predicted by the computer program which has been written for this purpose. If the difference between the experimental and predicted values is more than 15%, new correlation equations will be formulated.

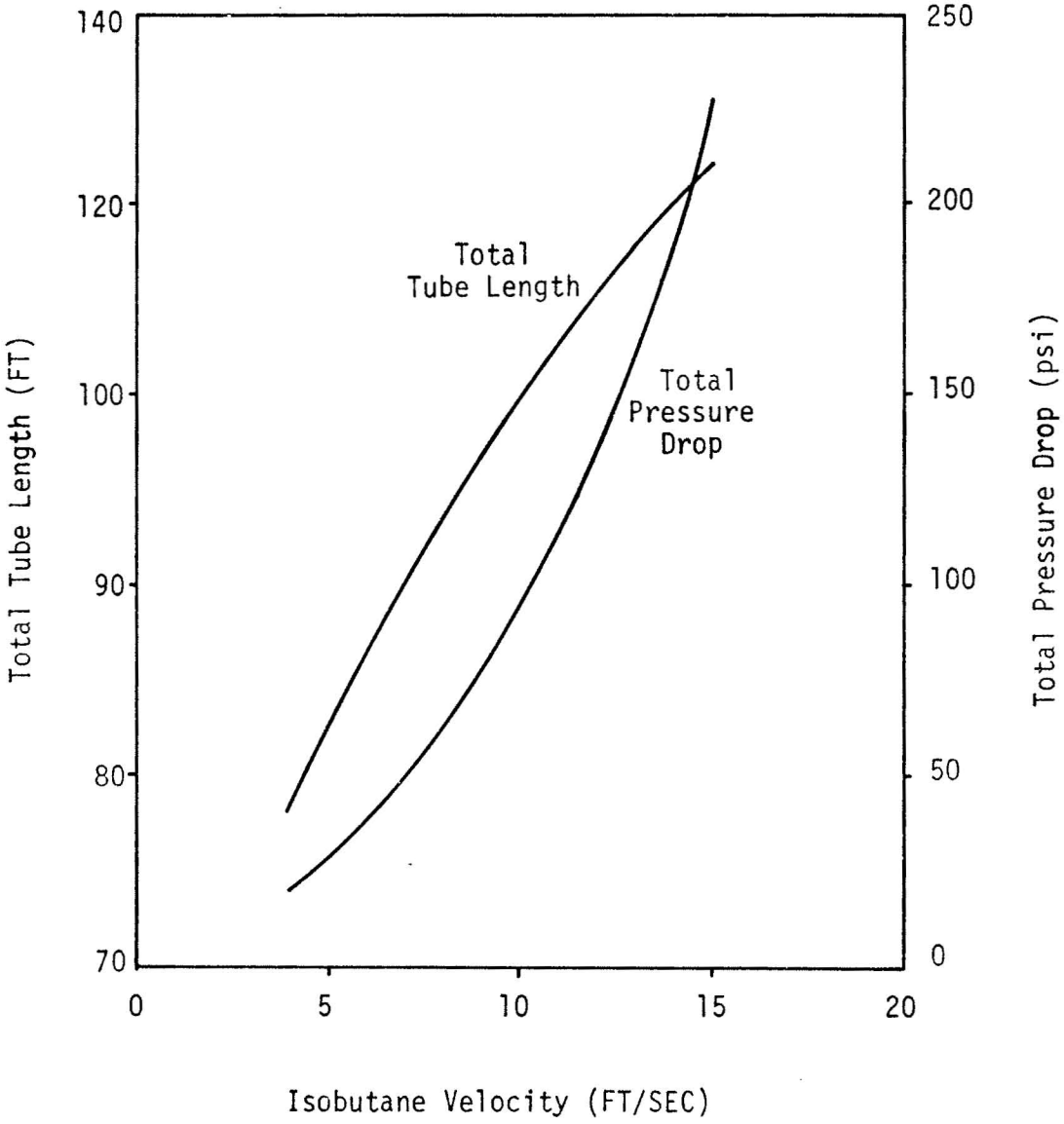

FIG. 3.6-13 EFFECT OF ISOBUTANE VELOCITY ON TUBE LENGTH AND PRESSURE DROP

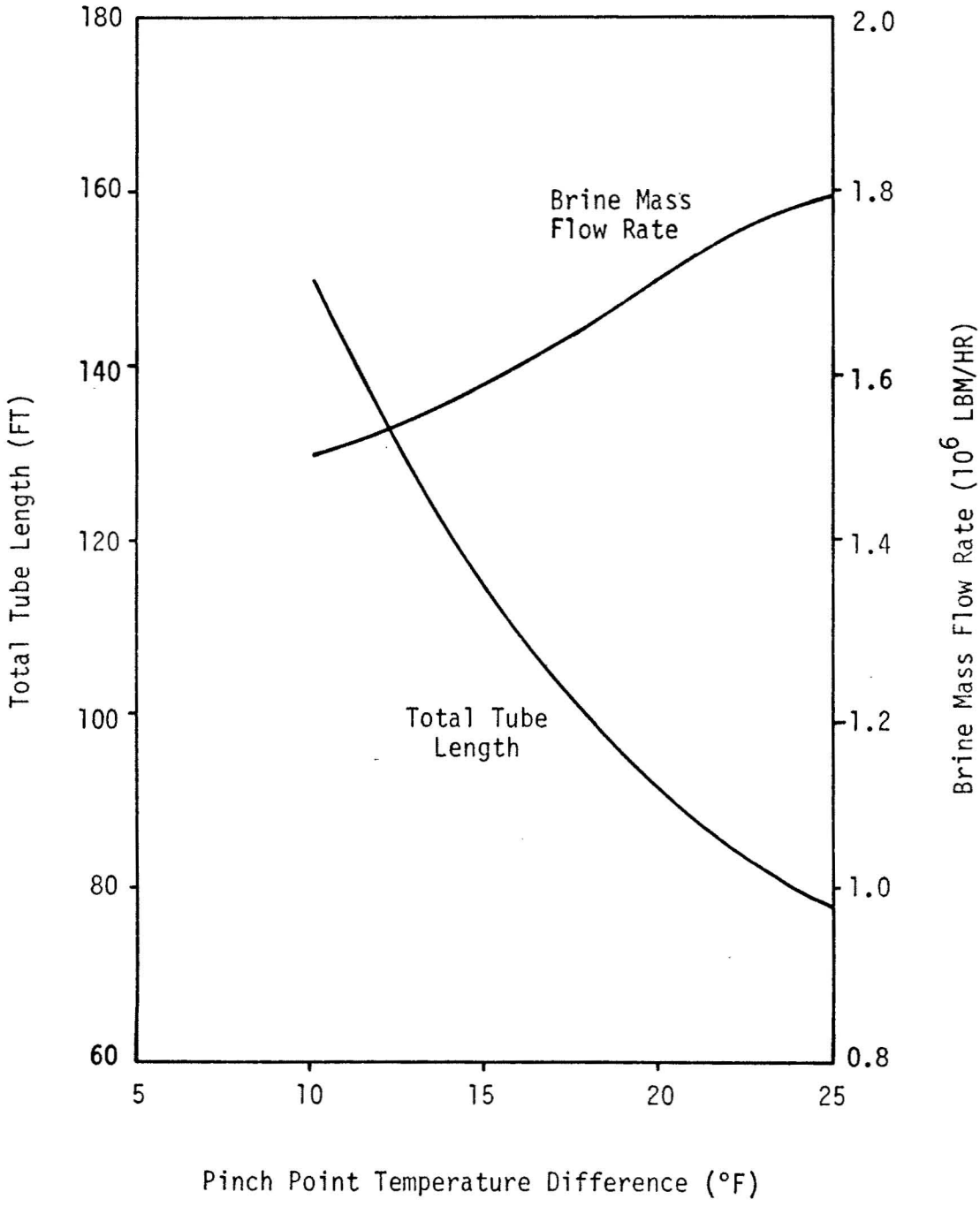

FIG. 3.6-14 THE EFFECT OF PINCH POINT TEMPERATURE DIFFERENCE ON TUBE LENGTH AND BRINE FLOW RATE

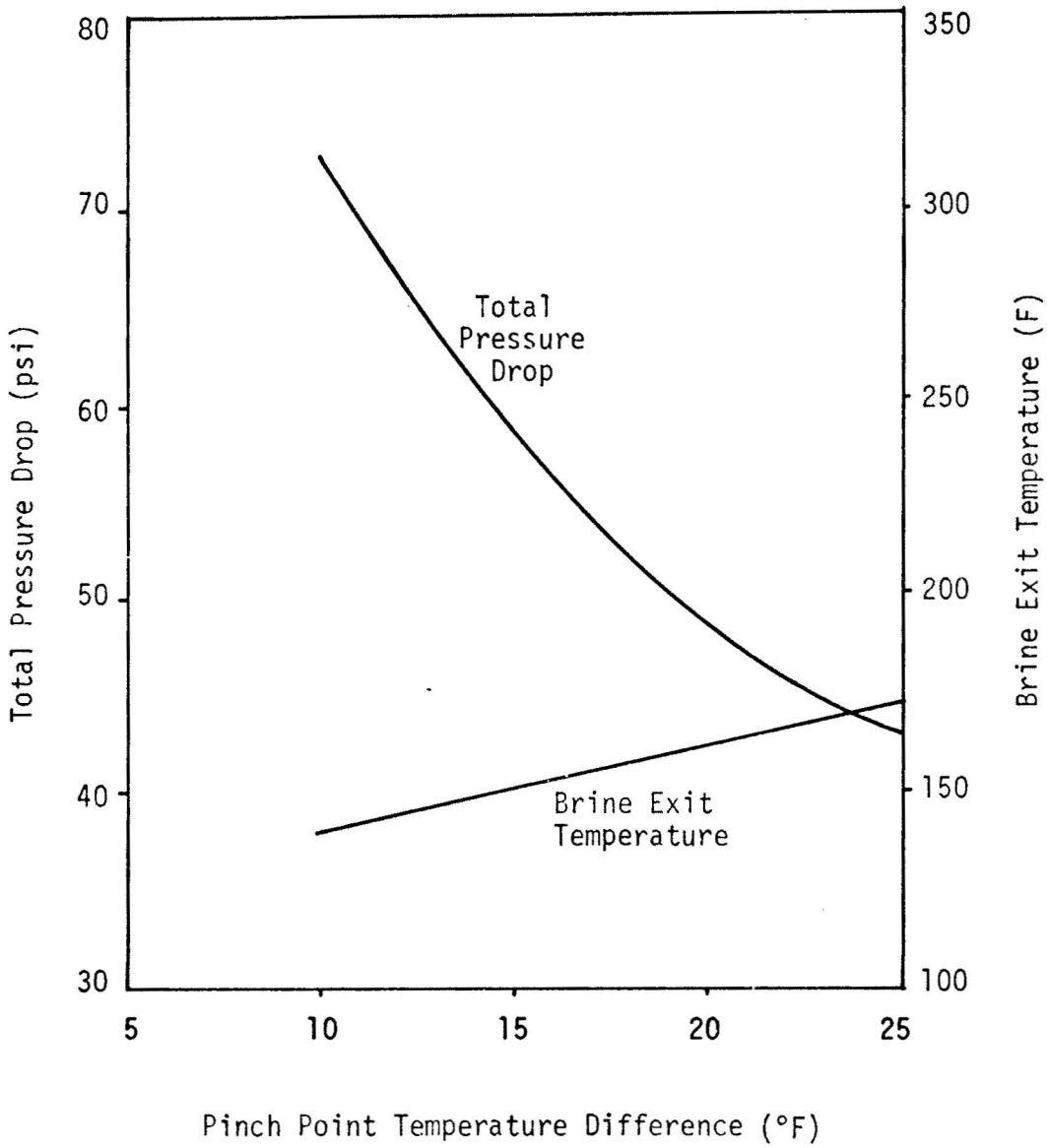

FIG. 3.6-15 THE EFFECT OF PINCH POINT TEMPERATURE DIFFERENCE ON PRESSURE DROP AND BRINE EXIT TEMPERATURE

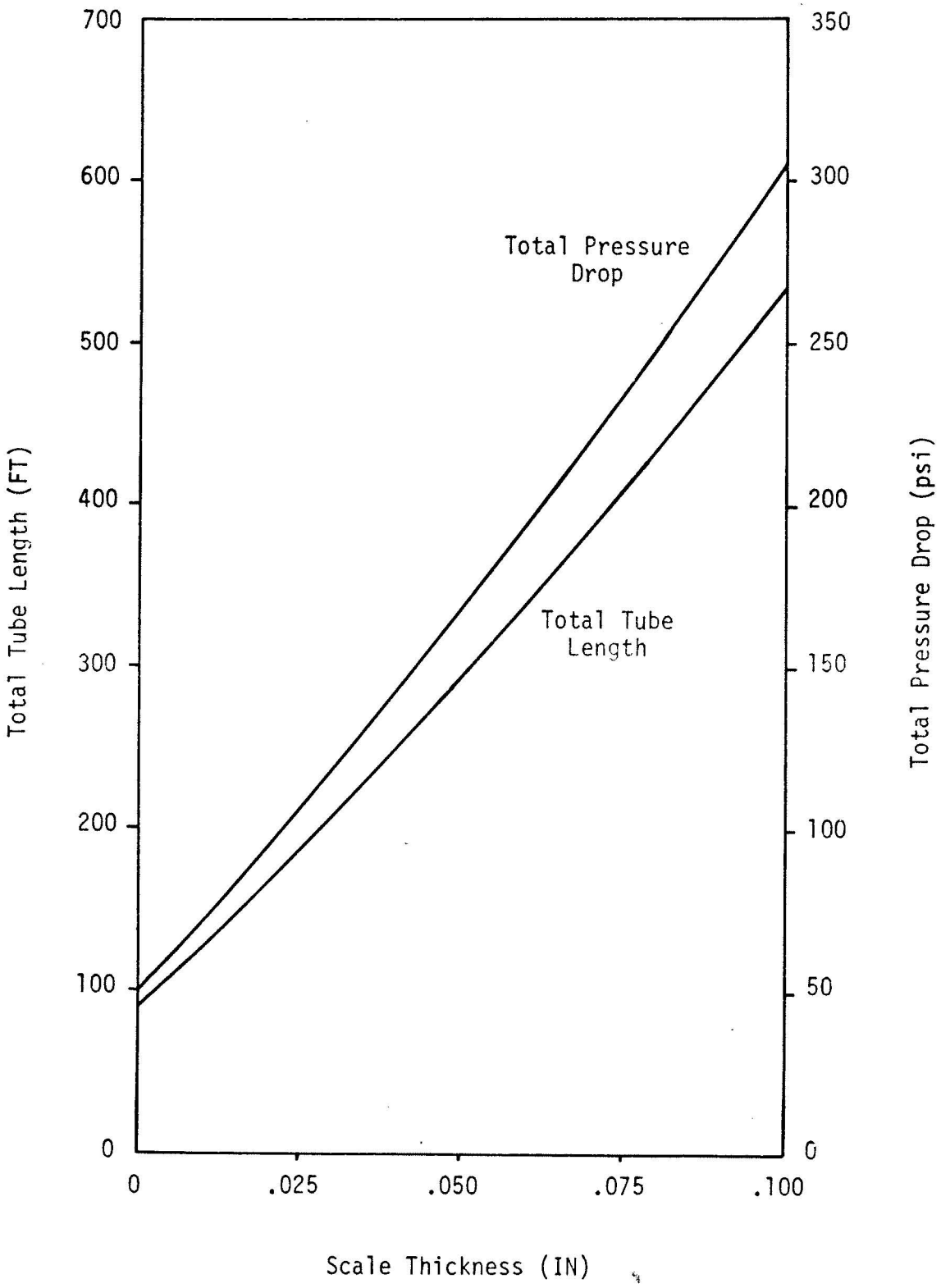

FIG. 3.6-16 THE EFFECT OF SCALE THICKNESS ON TUBE LENGTH AND PRESSURE DROP

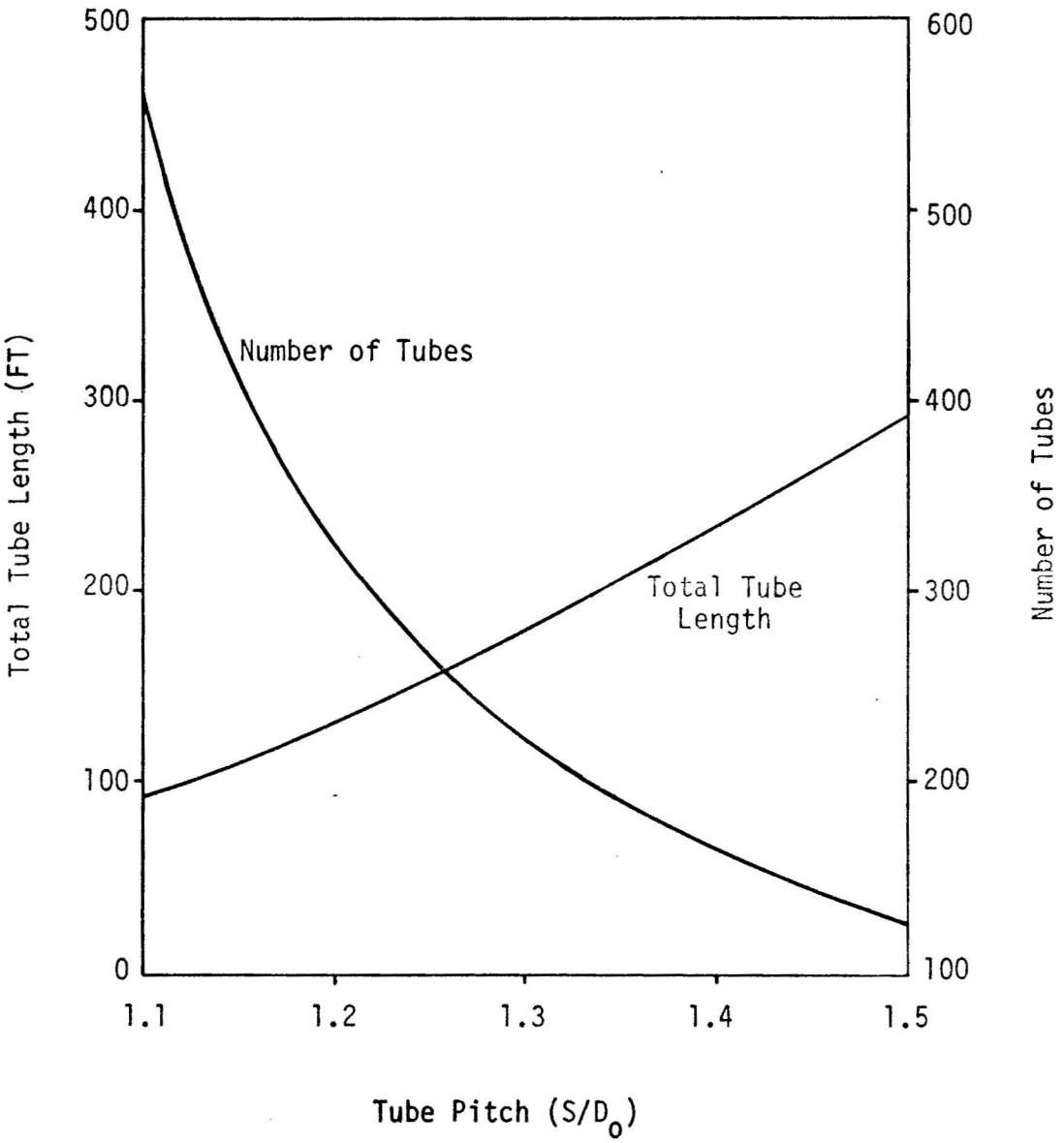

FIG. 3.6-17 THE EFFECT OF TUBE PITCH ON TUBE LENGTH AND NUMBER OF TUBES

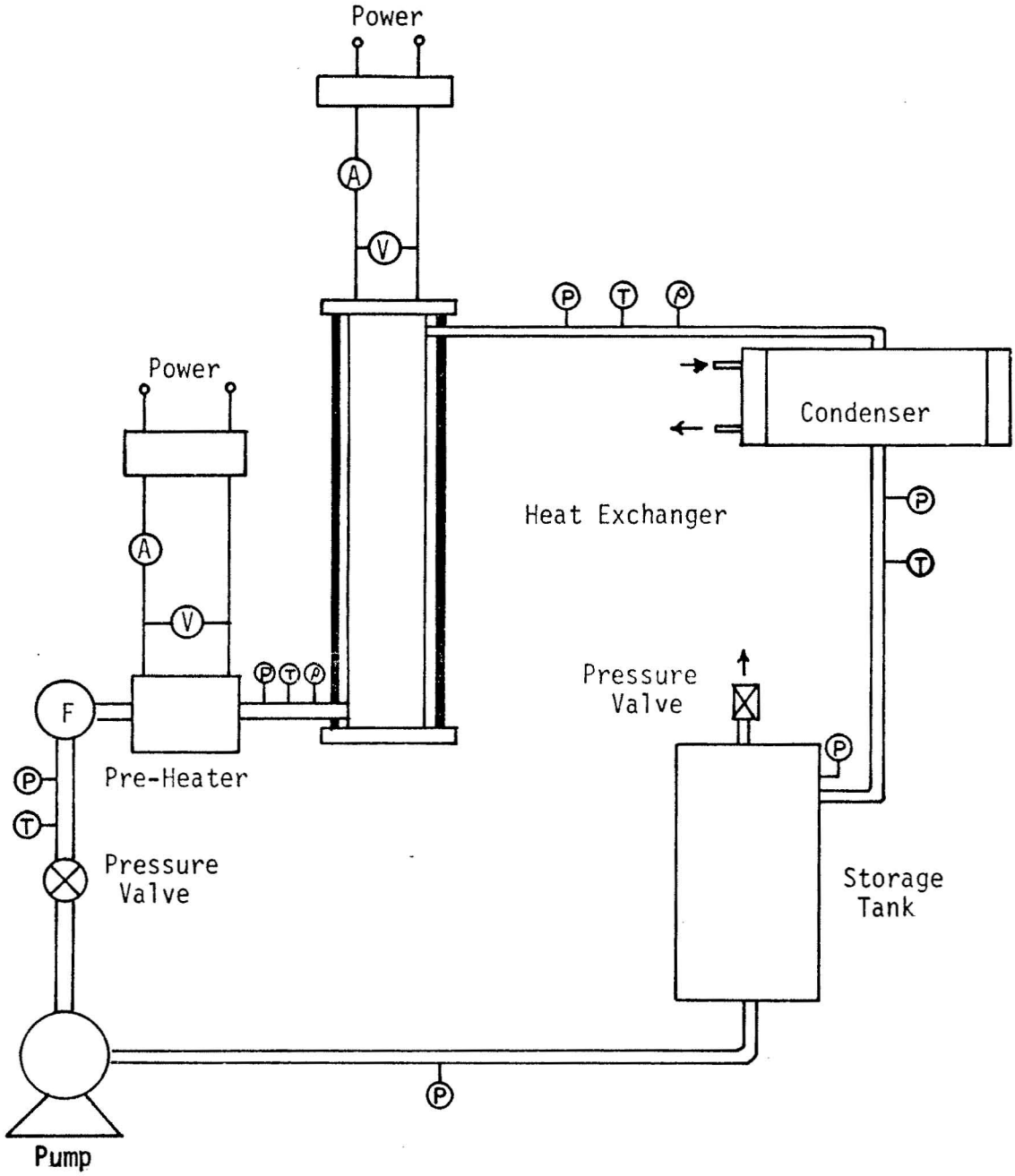

P - Pressure Meter
ρ - Density Meter
A - Ammeter
T - Temperature Meter
F - Flow Meter
V - Volt Meter

FIG. 3.6-18 SCHEMATIC OF EXPERIMENTAL TEST LOOP

Horizontal Heat Exchanger

Compute the average heat transfer coefficient and the pressure drop from the experimental data and formulate correlation equations for heat transfer and pressure drop. Comparison of the heat transfer and pressure drop correlation equations will be made between those for tube bundles and those for single horizontal tubes to obtain a correction factor which may be applied to the single tube equations to predict these values for tube bundles. The heat exchanger will be constructed with a pyrex glass cylinder in such a way that vapor generation and vapor passage can be observed. This information may be useful in selecting an optimum configuration for a horizontal heat exchanger.

Test Apparatus

Seven electrical tubular heaters (outside diameter = 0.496 inch, length = 51 5/8 inches, maximum power output per square inch = 40 watts) will be arranged with a triangular pitch of 0.744 inch in a pyrex cylinder (wall thickness = 0.25 inch, inside diameter = 2.25 inches) as shown in Fig. 3.6-19.

Power to the heaters will be supplied by the combination of a constant voltage transformer and a variable voltage transformer. Power input will be measured by a digital voltmeter and an ammeter.

A Consolidated Control analog-direct digital indicator will be used with the combination of copper-constantan thermocouples and turbine flow meter to measure the temperatures at various points and volumetric flow rate, respectively. Pressures will be measured by Bourden tube pressure gauges.

Investigations have been conducted to find a manufacturer of an instrument which will measure density or void fraction of vapor, but so far it has not been successful. In the event it is not possible to purchase the direct reading instrument, a throttling calorimeter will be used to measure the enthalpy of the vapor.

The condenser will be a single-shell two-tube pass type, and it will be constructed with 36 low finned tubes (outside diameter = 0.75 inch, fin height = 0.125 inch, length = 6 feet, number of fins per inch = 11) as depicted in Fig. 3.6-20. The tube side cooling water will be cooled by a five-ton water-cooled water chiller. Condensed Freon will be stored in a stainless steel or copper tank.

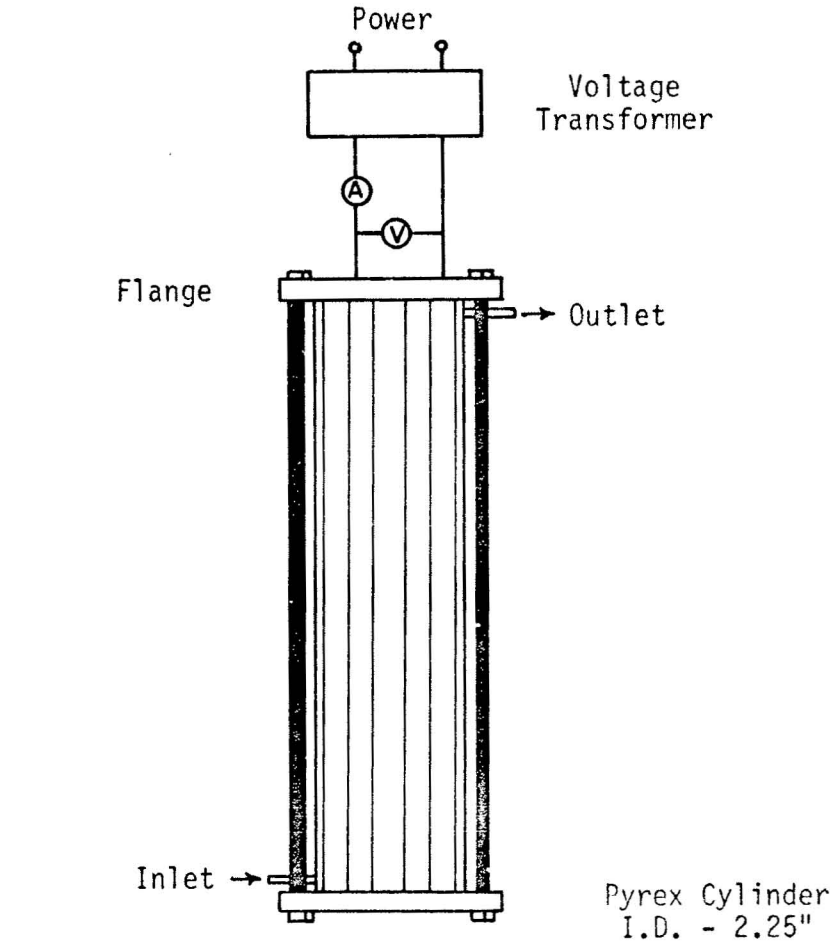

FIG. 3.6-19 LAYOUT OF HEAT EXCHANGER TEST SECTION

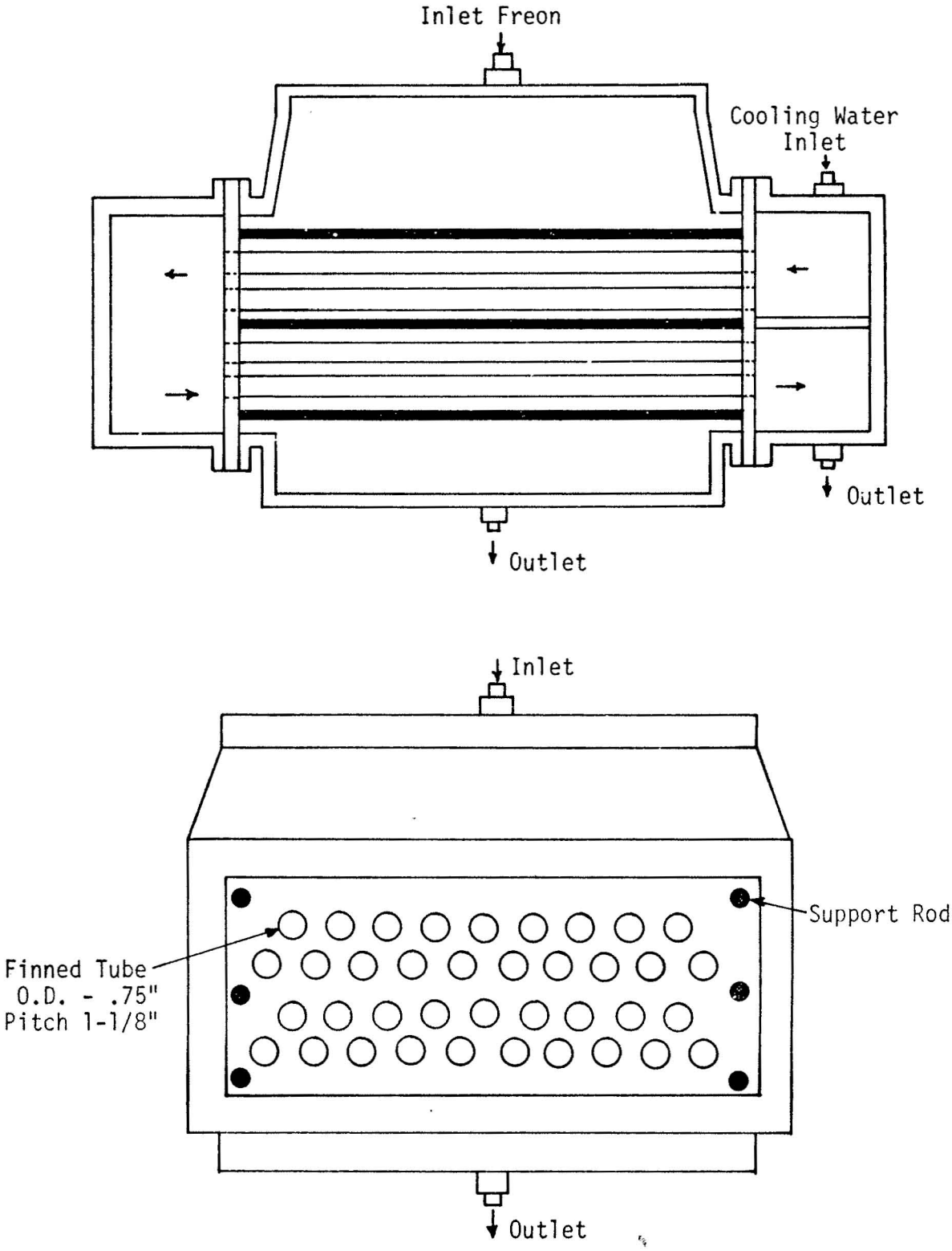

FIG. 3.6-20 LAYOUT OF CONDENSER

C. Future Work

During the next quarterly period, the following work will be undertaken:

1. Survey of availability of components which can be used in a regenerative binary fluid cycle power plant.
2. Construction of components will continue and assembly and check out of experimental heat transfer loop will be initiated.

D. References

1. Harned, H. S. and Owen, B., *THE PHYSICAL CHEMISTRY OF ELECTROLYTIC SOLUTIONS*, 3rd ed., Reinhold Publishing Corporation, New York, 1958.

2. Robinson, R. A. and Stokes, R. H., *ELECTROLYTE SOLUTIONS*, 2nd ed., Butterworth and Company, London, 1959.

3. Fabuss, B. M. and Korosi, A., "Properties of Sea Water and Aqueous Electrolyte Solutions containing NaCl, KCl, Na_2SO_4 and $MgSO_4$," Report submitted to the Office of Saline Water by Monsanto Research Corporation, 1968.

4. Bromley, L. A., "Properties of Seawater and Its Concentrates and Related Solutions at Temperatures up to 400°F," Progress Report No. 747, Office of Saline Water, 1972.

5. Liu, C. T. and Lindsay, W. T., "Thermodynamic Properties of Aqueous Solutions at High Temperatures," Progress Report No. 722, Office of Saline Water, 1971.

6. Chou, J. C. S., "Thermal Properties of Sea Water," Technical Report No. 49, Water Resources Research Center, University of Hawaii, 1971.

7. Belteky, L., "Development and Utilization of Thermal Waters in Hungary," *GEOTHERMICS*, Vol. 1, No. 3, 1972, p. 103-112.

8. Ellis, A. J., "The Solubility of Calcite in Carbon Dioxide Solutions," *AMERICAN JOURNAL OF SCIENCE*, Vol. 257, 1959, p. 354-365.

9. Ellis, A. J., "The Solubility of Calcite in Sodium Chloride Solutions at High Temperatures," *AMERICAN JOURNAL OF SCIENCE*, Vol. 261, 1963, p. 259-267.

10. Ellis, A. J., and Golding, R. M., "The Solubility of Carbon Dioxide above 100°C in Water and in Sodium Chloride Solutions," *AMERICAN JOURNAL OF SCIENCE*, Vol. 261, 1963, p. 47-61.

11. Malinin, S. D., "An Experimental Investigation of the Solubility of Calcite and Witherite under Hydrothermal Conditions," *GEOCHEMISTRY*, No. 7, 1963, p. 651-667.

12. Morse, John W., "Dissolution Kinetics of Calcium Carbonate in Sea Water III," *AMERICAN JOURNAL OF SCIENCE*, Vol. 274, 1974, p. 97-107.

13. Rogers Engineering Company, "Process Description of the EFP System Model," Unpublished paper, San Francisco, 1973.